Supplementary information for

Seed-Mediated Colloidal Synthesis of Multimetallic and High-Entropy Alloy Nanocrystal Libraries with Enhanced Catalytic Performance

Jinwon Oh,[1] Shuang Han,[2] Evan J. Gardner,[3] Rohan Parekh,[1] Audrey Dannar,[4] Pin-Hung Chung,[1] Kaifeng Zheng,[5] Anna Mian,[6] Karen C. Bustillo,[7] Christian Reece,[4] Anatoly I. Frenkel,[5, 8] Colin Ophus,[1] Carlos Lizandara-Pueyo,[2,9] Sandip De,[2, *] Matteo Cargnello[3, *]

[1]*Department of Materials Science and Engineering, Stanford University, Stanford, CA 94305, USA*

[2]*BASF SE, Carl-Bosch-Straße 38, 67056, Ludwigshafen, Germany*

[3]*Department of Chemical Engineering and SUNCAT Center for Interface Science and Catalysis, Stanford University, Stanford, CA 94305, USA*

[4]*Rowland Institute at Harvard, Harvard University, Cambridge, MA 02142, USA*

[5]*Department of Materials Science and Chemical Engineering, Stony Brook University, Stony Brook, NY, 11794, USA*

[6]*TESCAN Tempe, LLC., Tempe, Arizona 85281, USA*

[7]*National Center for Electron Microscopy, Molecular Foundry, Lawrence Berkeley National Laboratory, Berkeley, CA 94720, USA*

[8]*Division of Chemistry, Brookhaven National Laboratory, Upton, NY, 11973, USA*

[9]*California Research Alliance (CARA), BASF Corporation, Berkeley, CA 94720, USA*

Corresponding authors: mcargn@stanford.edu, sandip.de@basf.com

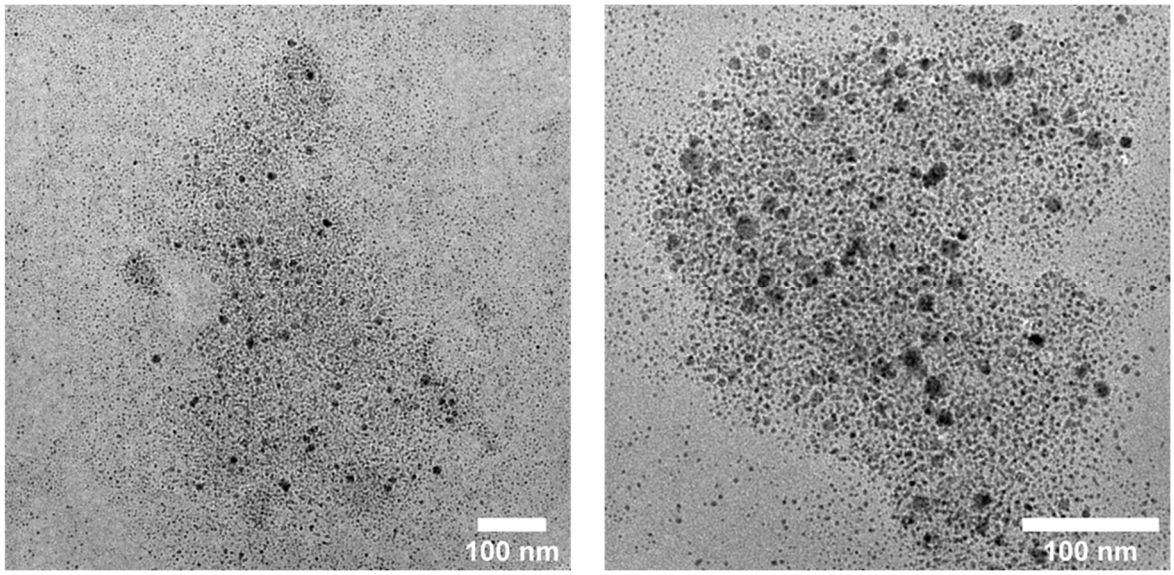

Figure S1. BF-TEM images of products of one-pot synthesis of PtCoNiCuZn.

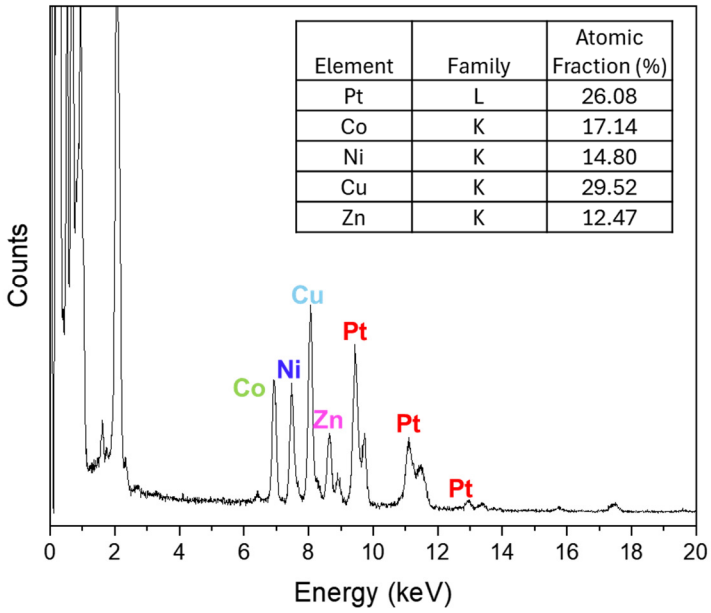

Figure S2. EDS spectrum and calculated atomic fraction of samples in Figure 1d. Au signals are from the grid.

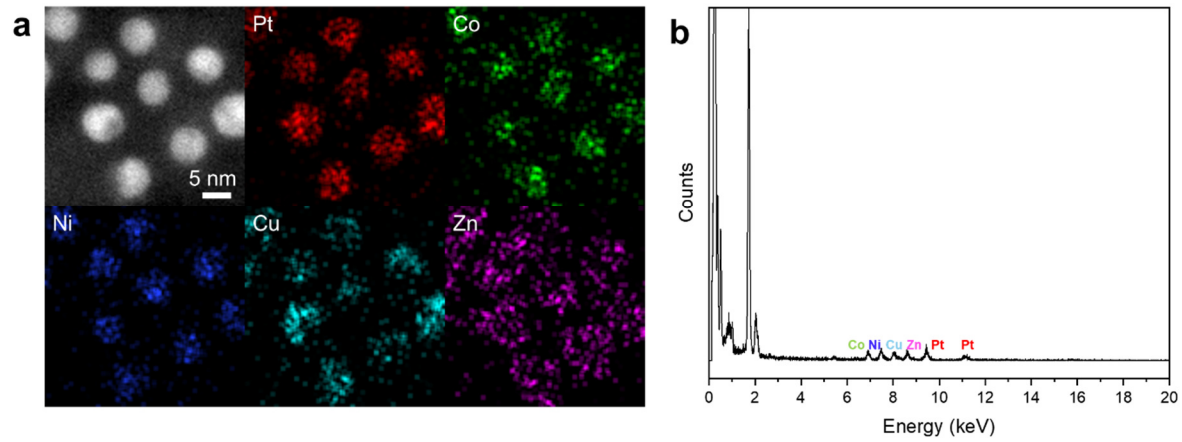

Figure S3. (a) HAADF-STEM image and corresponding EDS maps of PtCoNiCuZn nanocrystals synthesized at 350 °C for 4 h. (b) EDS spectrum corresponding to panel (a).

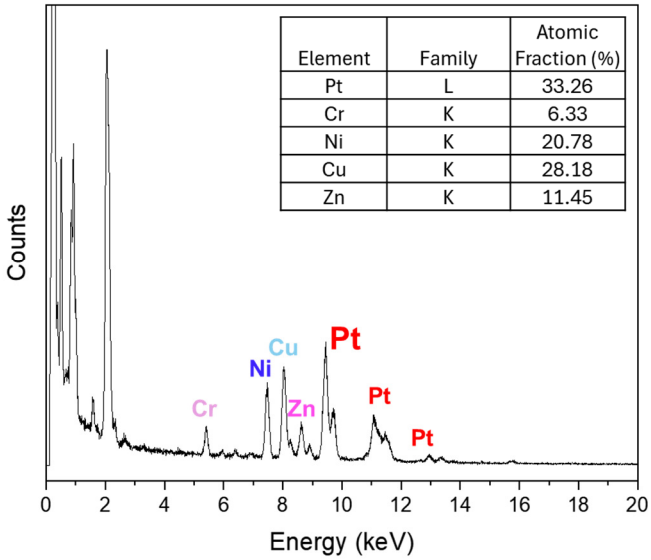

Figure S4. EDS spectrum of EDS maps in Figure 2d.

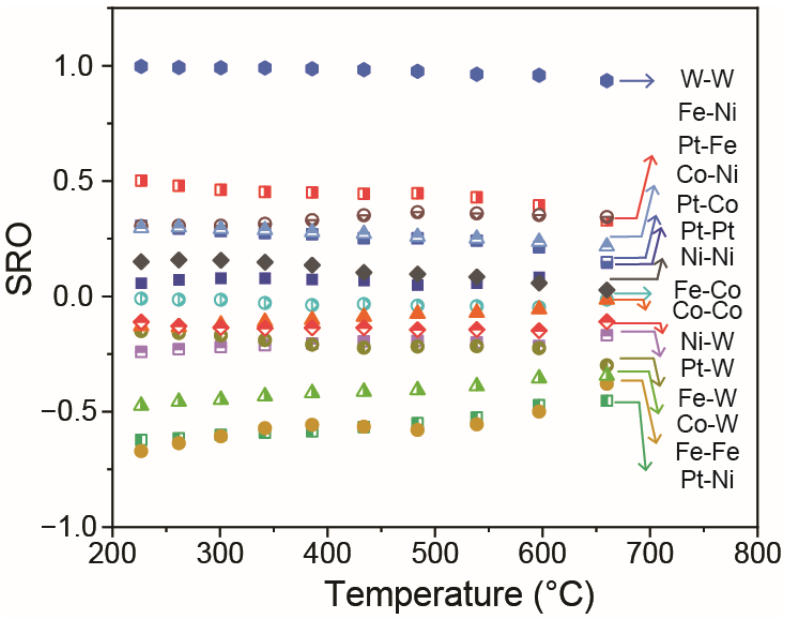

Figure S5. SRO of all possible atomic pairs in PtFeCoNiW at different temperatures

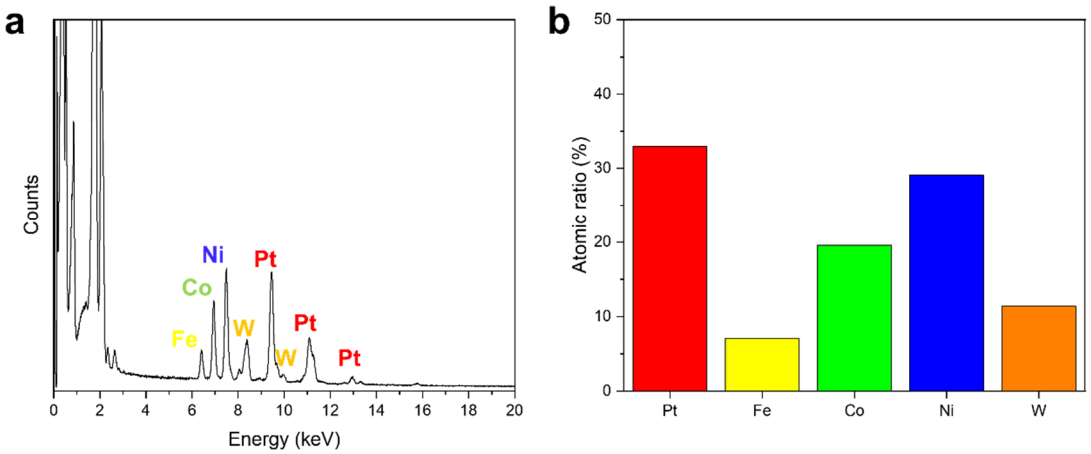

Figure S6. (a) STEM-EDS spectrum of PtFeCoNiW nanocrystals in Figure 2e. (Cu signal is from the TEM grid and Zr signal is from the system.) (b) Atomic ratio calculation from the EDS spectrum in Figure S6a.

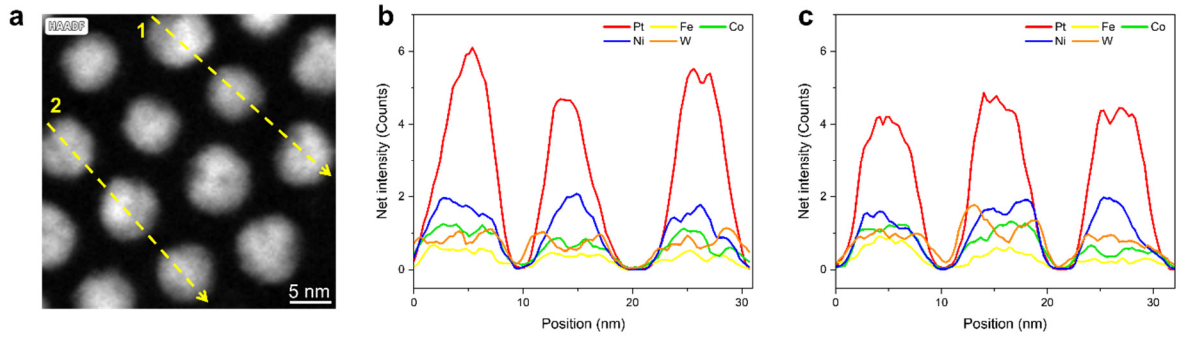

Figure S7. (a) HAADF-STEM image of PtFeCoNiW nanocrystals. STEM-EDS line scan profiles of line 1 (b) and line 2 (c) in Figure S7a.

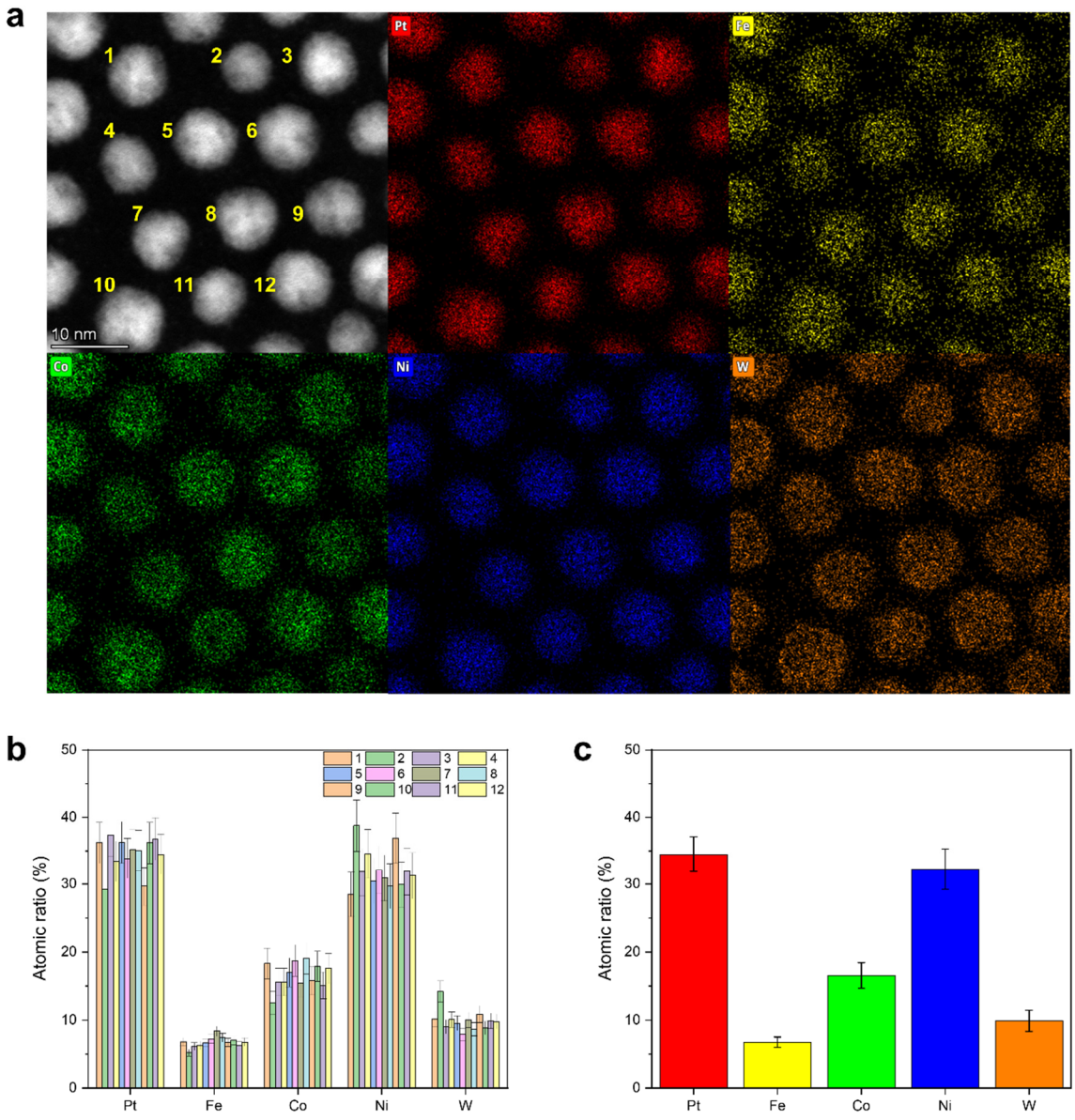

Figure S8. (a) HAADF-STEM image of PtFeCoNiW nanocrystals with numbering of nanocrystals and corresponding EDS maps (b) Atomic ratio quantification of 12 nanocrystals in Figure S8a. (c) Average elemental distribution of 12 nanocrystals in Figure S8a.

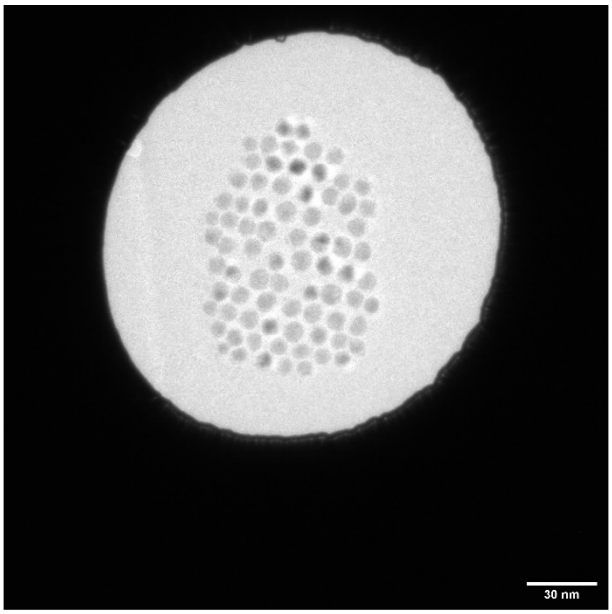

Figure S9. BF-TEM image of selected area in Figure 2g.

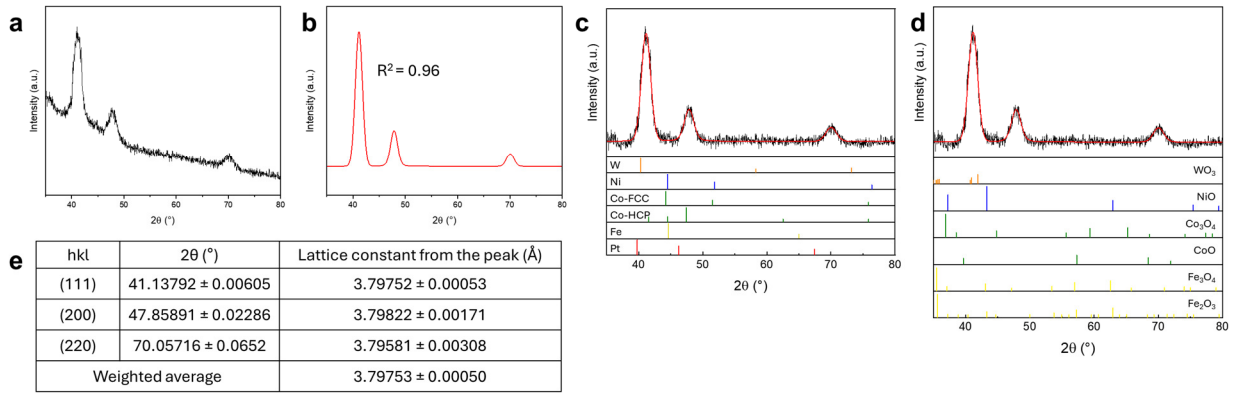

e

hkl	2θ (°)	Lattice constant from the peak (Å)
(111)	41.13792 ± 0.00605	3.79752 ± 0.00053
(200)	47.85891 ± 0.02286	3.79822 ± 0.00171
(220)	70.05716 ± 0.0652	3.79581 ± 0.00308
Weighted average		3.79753 ± 0.00050

Figure S10. (a) XRD pattern without background subtraction. (b) Fitted XRD spectrum corresponding to panel (a). XRD analysis of PtFeCoNiW nanocrystals with reference peaks of metals (c) and metal oxides (d). (e) Fitting results with the calculated lattice constant.

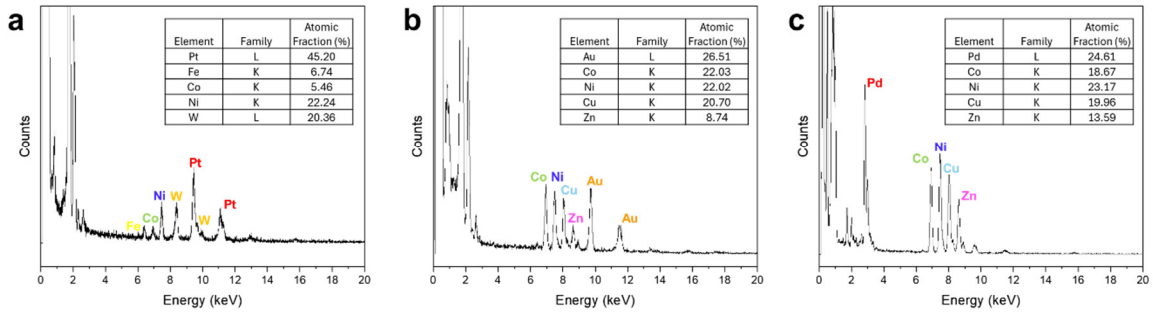

Figure S11. EDS spectra of nanocrystals in Figure 3. (a) PtFeCoNiW, (b) AuCoNiCuZn, and (c) PdCoNiCuZn.

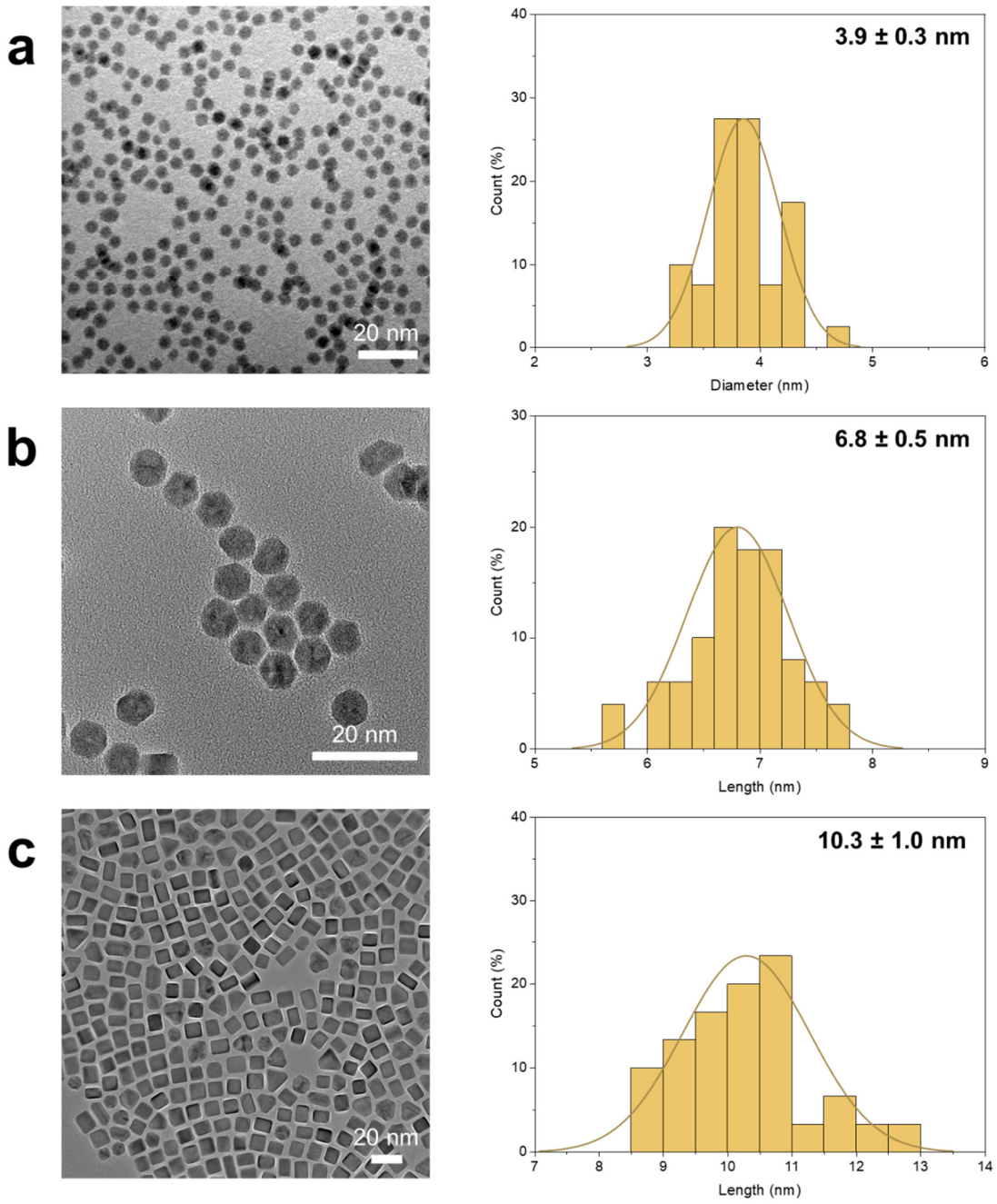

Figure S12. BF-TEM images of various seed Pt nanocrystals and their size distributions. (a) BF-TEM image of small Pt nanocrystals and their size distribution. (b) BF-TEM image of faceted Pt nanocrystals and their size distribution. (c) BF-TEM image of cubic Pt nanocrystals and their size distribution.

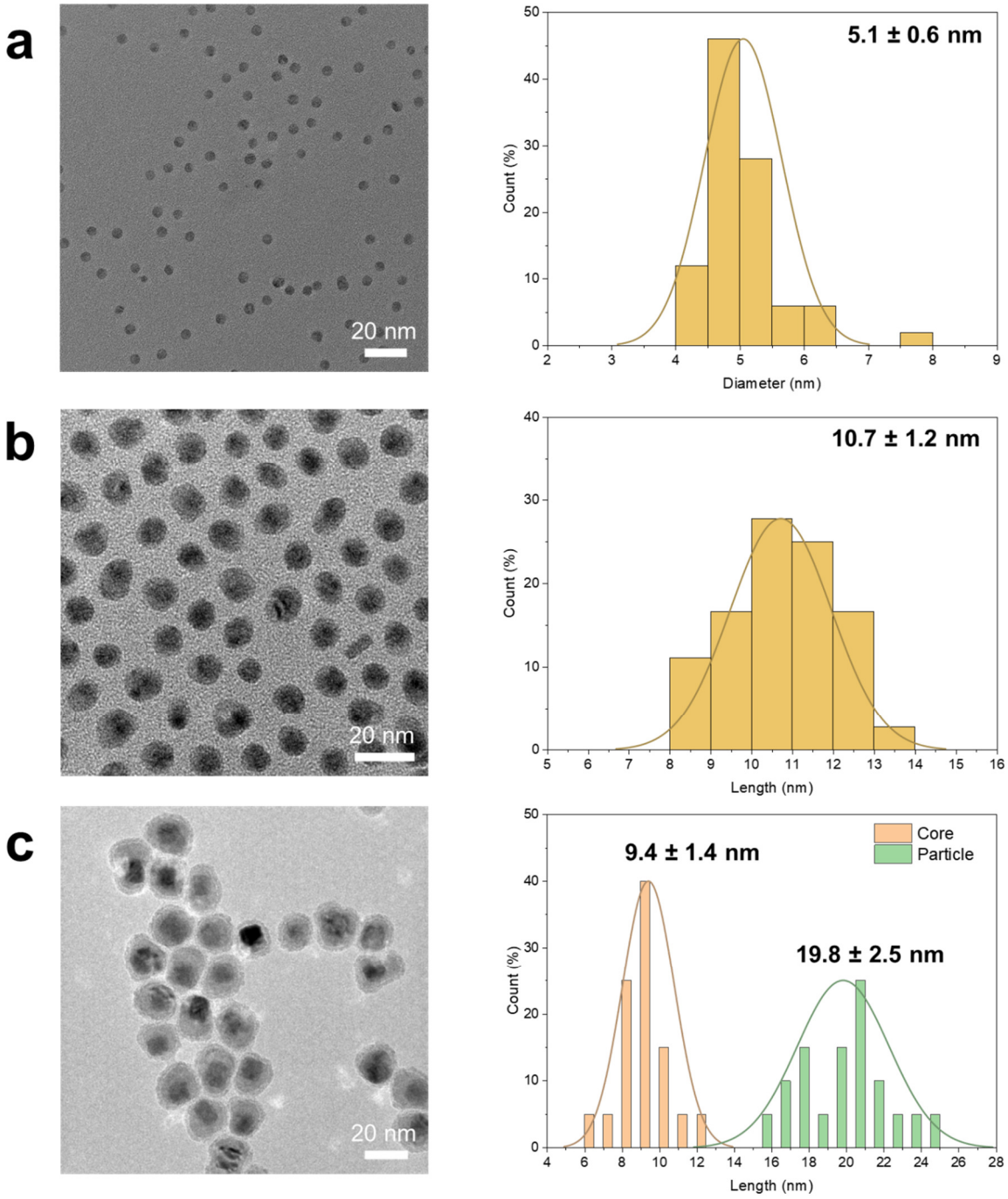

Figure S13. BF-TEM images of PtCoNiCuZn nanocrystals and their size distributions. (a) BF-TEM image of PtCoNiCuZN nanocrystals grown from smaller seeds and their size distribution. (b) BF-TEM image of PtCoNiCuZn nanocrystals grown from faceted seeds and their size distribution. (c) BF-TEM image of PtCoNiCuZn nanocrystals grown from cubic-shaped seeds and their size distribution.

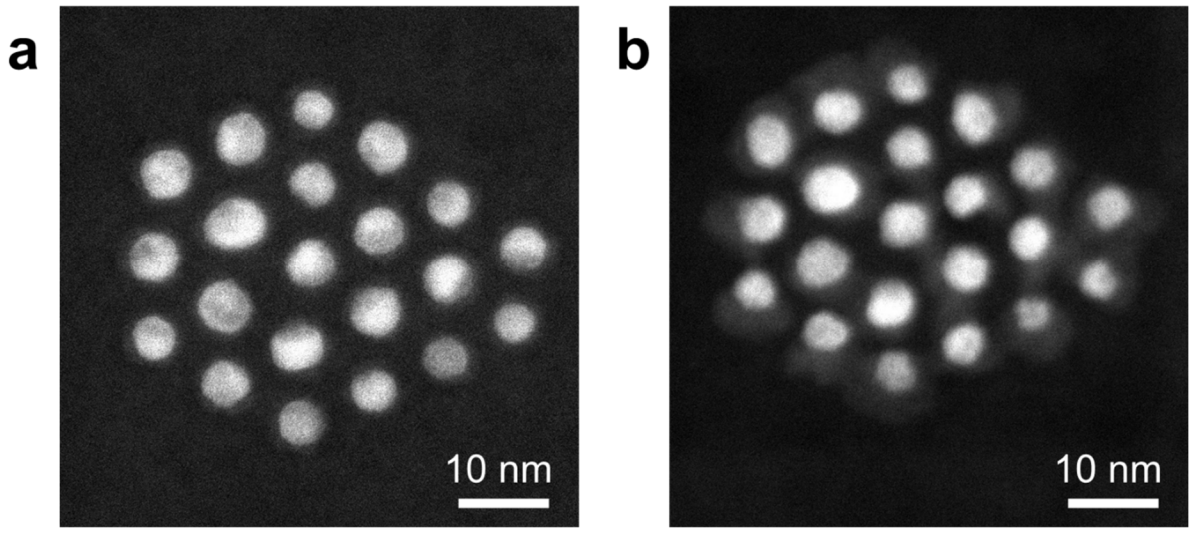

Figure S14. HAADF-STEM images of PtCoNiCuZN nanocrystals grown from smaller seeds before (a) and after (b) EDS collection.

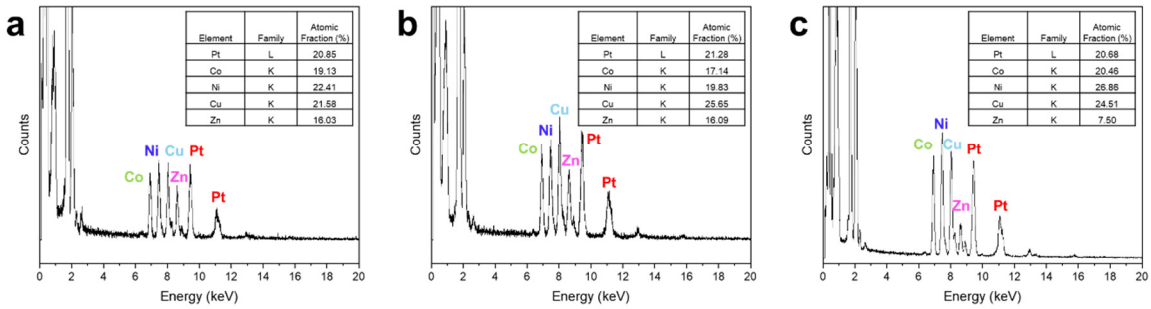

Figure S15. EDS spectra of PtCoNiCuZn nanocrystals in Figure 4. (a) PtCoNiCuZn nanocrystals grown from smaller seeds. (b) PtCoNiCuZn nancorystals grown from faceted seeds. (c) PtCoNiCuZn nanocrystals grown from cubic-shaped seeds.

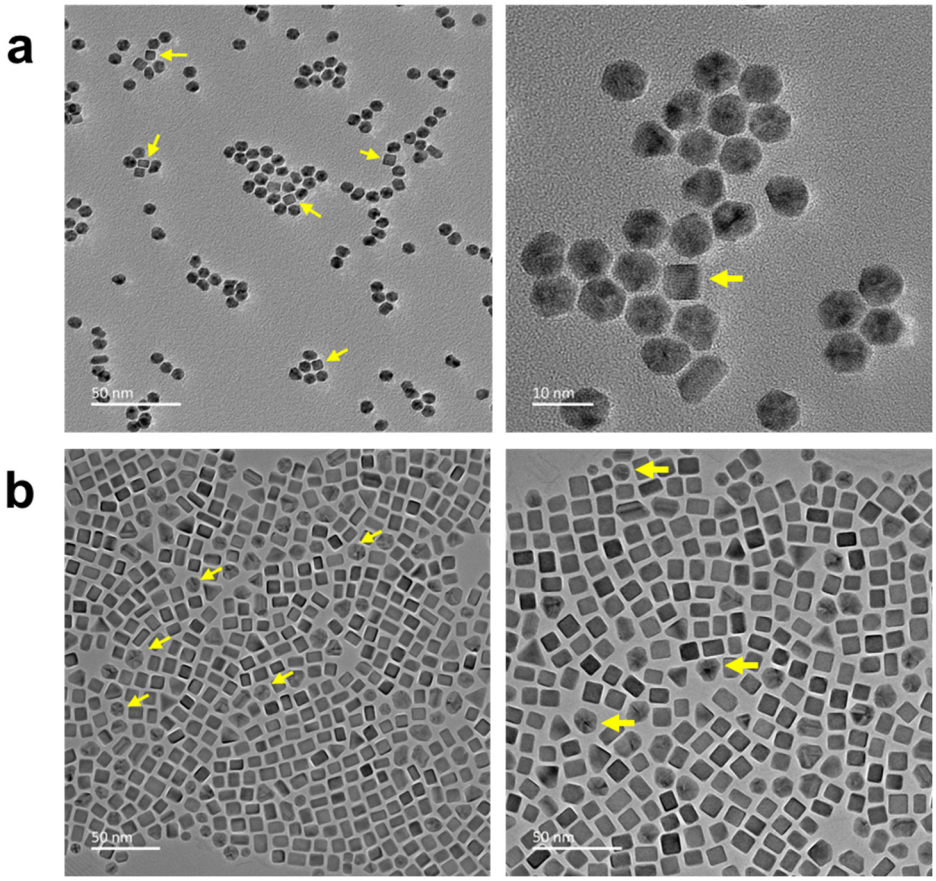

Figure S16. (a) BF-TEM image of faceted Pt seed nanocrystals, with yellow arrows indicating the subset of cubic nanocrystals. (b) BF-TEM image of cubic Pt nanocrystals, with yellow arrows indicating the subset of faceted nanocrystals.

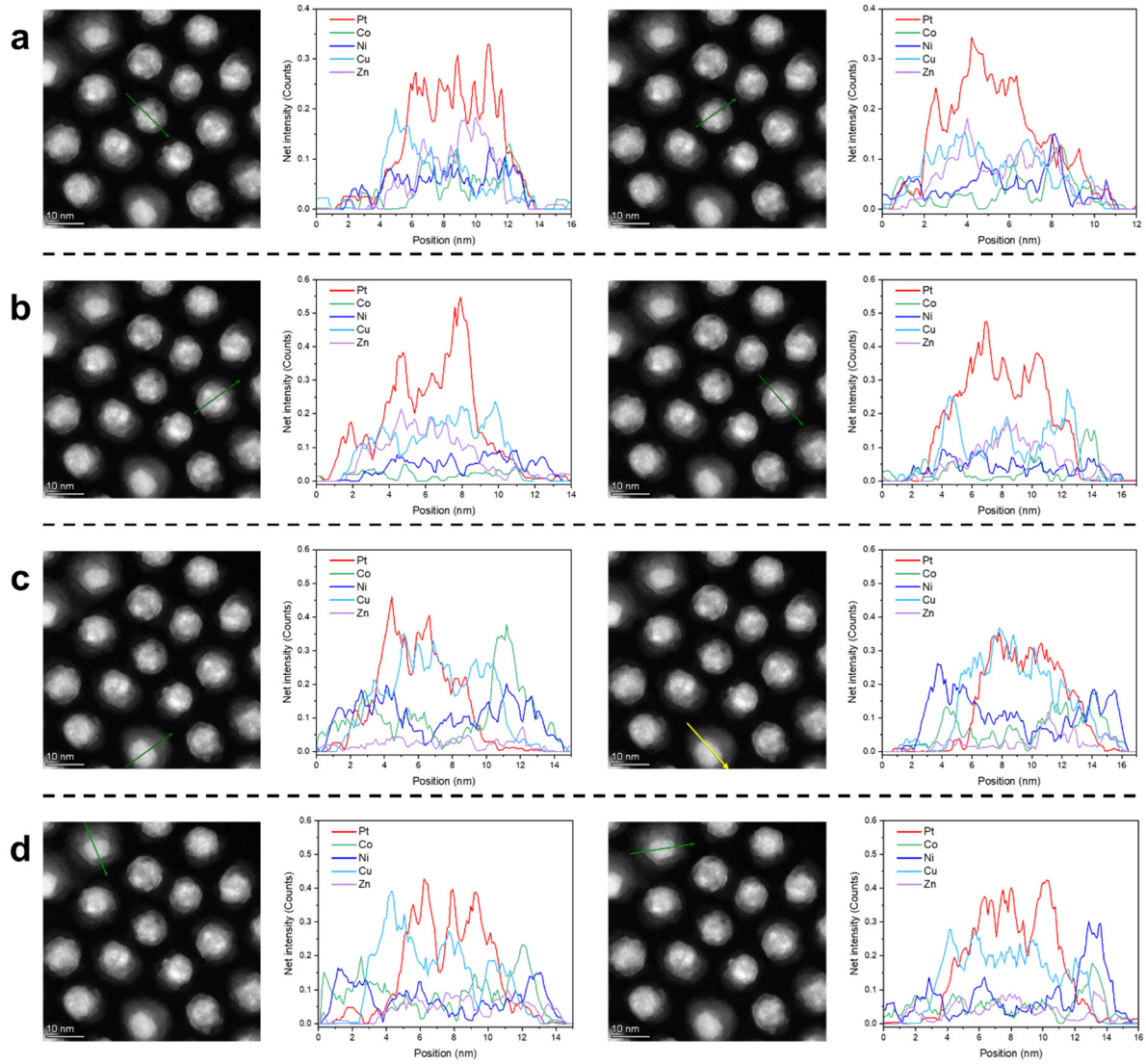

Figure S17. EDS line scan analysis of PtCoNiCuZn nanocrystals synthesized from a faceted nanocrystal batch. (a-b) PtCoNiCuZn nanocrystals from faceted seeds. (c-d) PtCoNiCuZn nanocrystals from cubic-shaped seeds. For the line scan analysis, the EDS map data from Figure 4d were used, and signals from nine pixels were averaged.

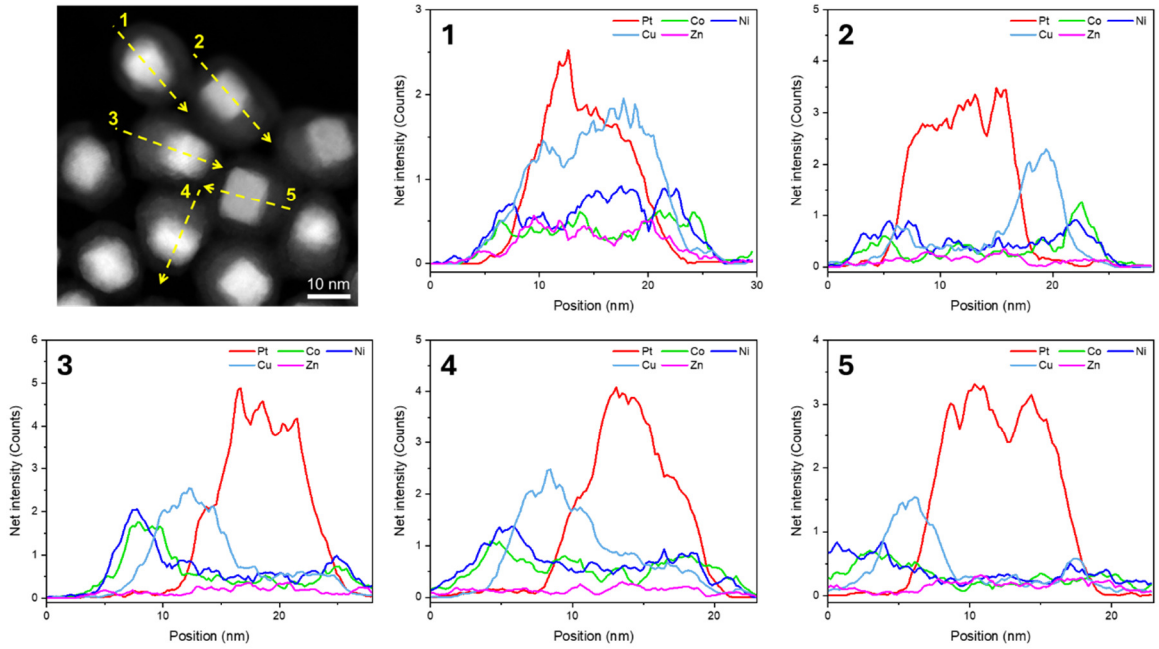

Figure S18. EDS line scan analysis of PtCoNiCuZn nanocrystals synthesized from a cubic nanocrystal batch. The nanocrystal labeled [1] originated from a faceted nanocrystal, while the remaining nanocrystals were derived from cubic seeds. For the line scan analysis, the EDS map data from Figure 4f were used, and signals from seven pixels were averaged.

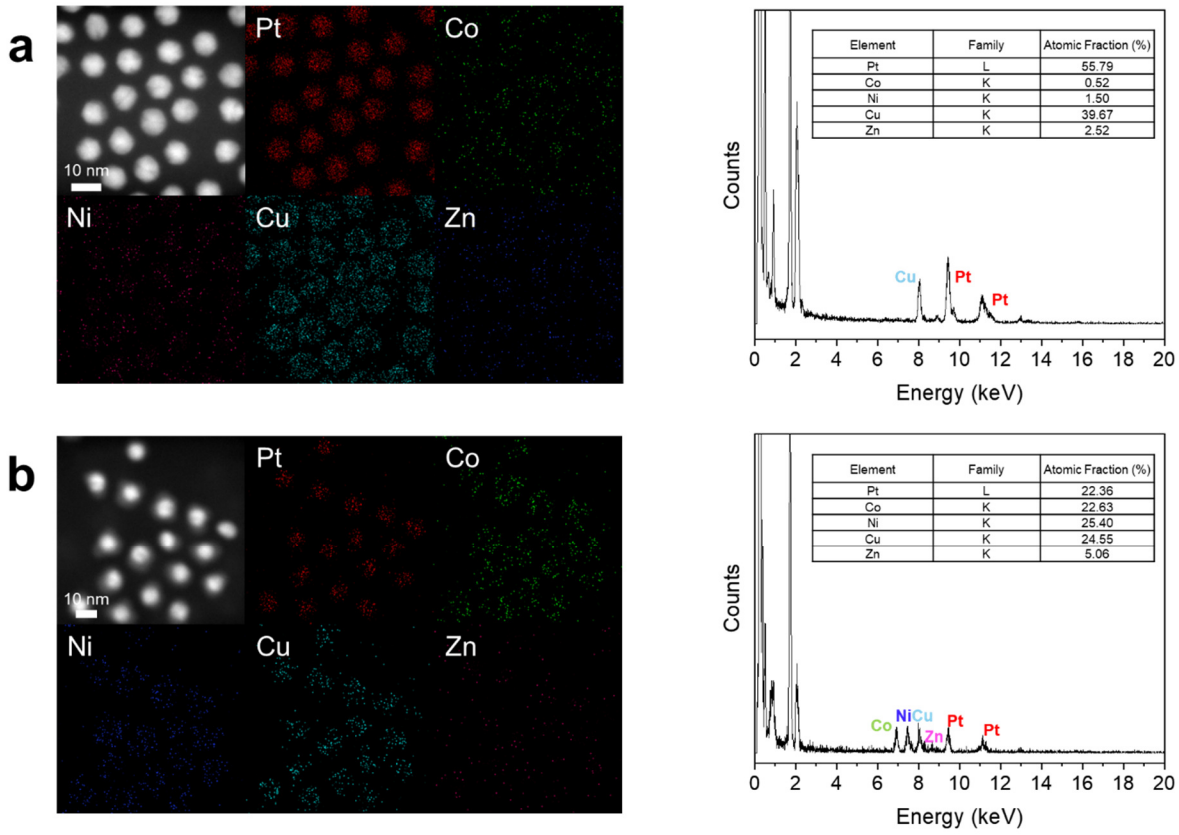

Figure S19. HAADF-STEM images, corresponding EDS maps, and spectra with calculated atomic fractions of PtCoNiCuZn nanocrystals synthesized from faceted seeds and collected at (a) 190 °C and (b) 250 °C.

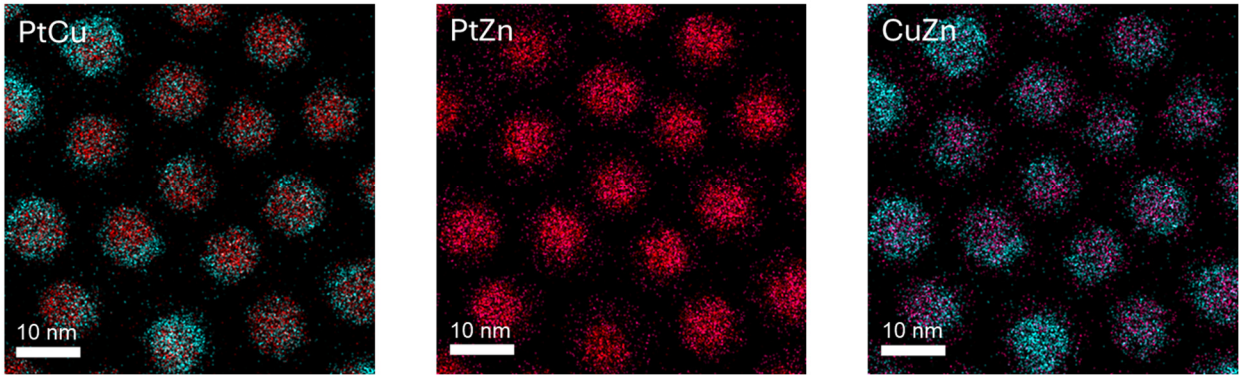

Figure S20. EDS overlays of Pt-Cu, Pt-Zn, and Cu-Zn signals for PtCoNiCuZn nanocrystals synthesized from faceted seeds.

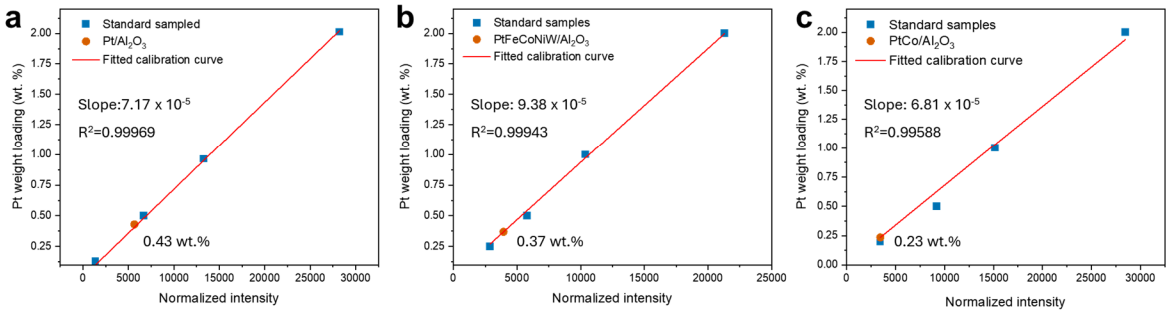

Figure S21. XRF measurements of Pt/Al_2O_3 (a), $PtFeCoNiW/Al_2O_3$ (b), and $PtCo/Al_2O_3$ (c).

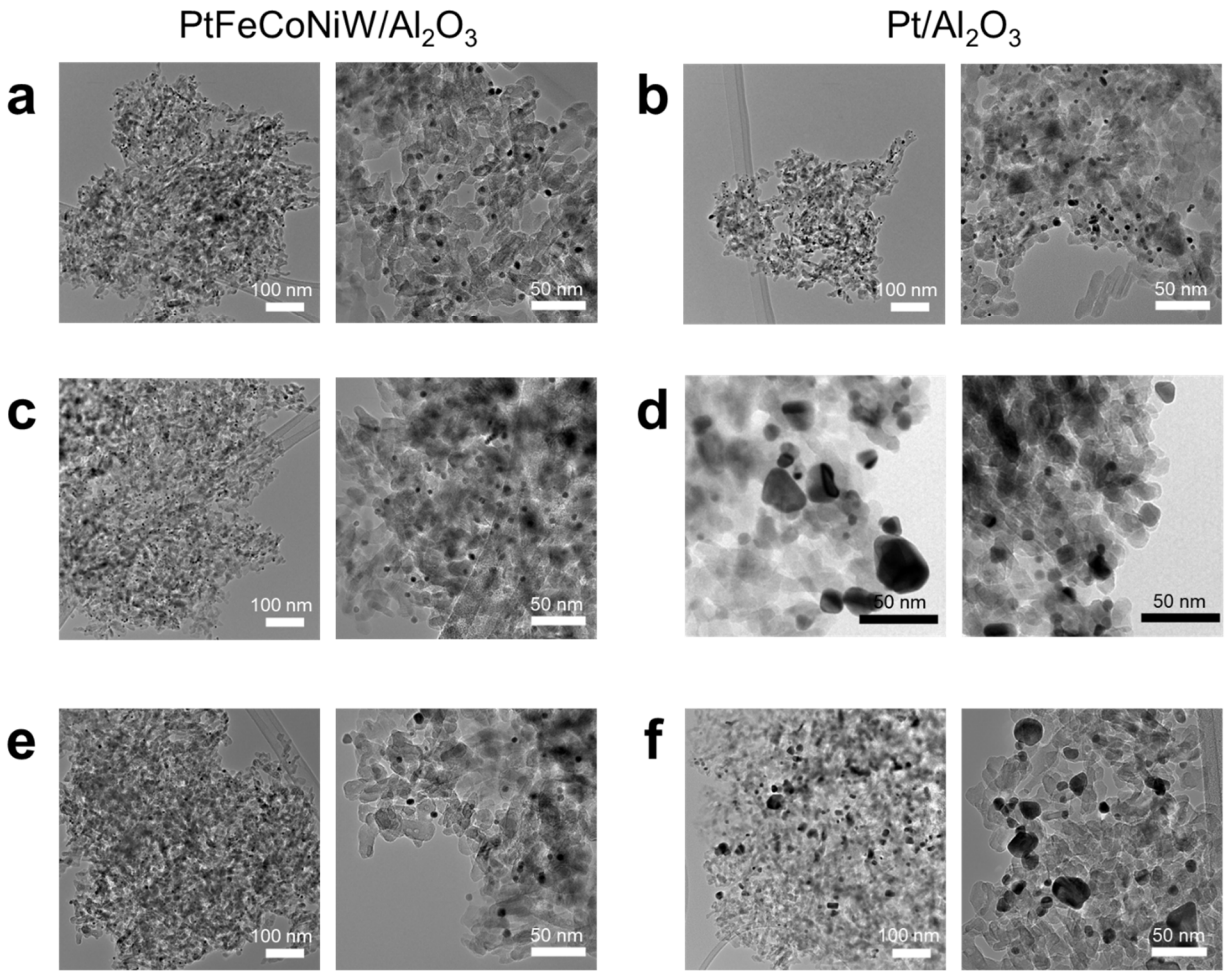

Figure S22. BF-TEM images of $PtFeCoNiW/Al_2O_3$ and Pt/Al_2O_3 after thermal treatment and aging. After thermal treatment for ligand removal: (a) $PtFeCoNiW/Al_2O_3$ and (b) Pt/Al_2O_3. After hydrothermal aging at 600 °C for 6 hours (c) (d) and at 650 °C for 6 hours.

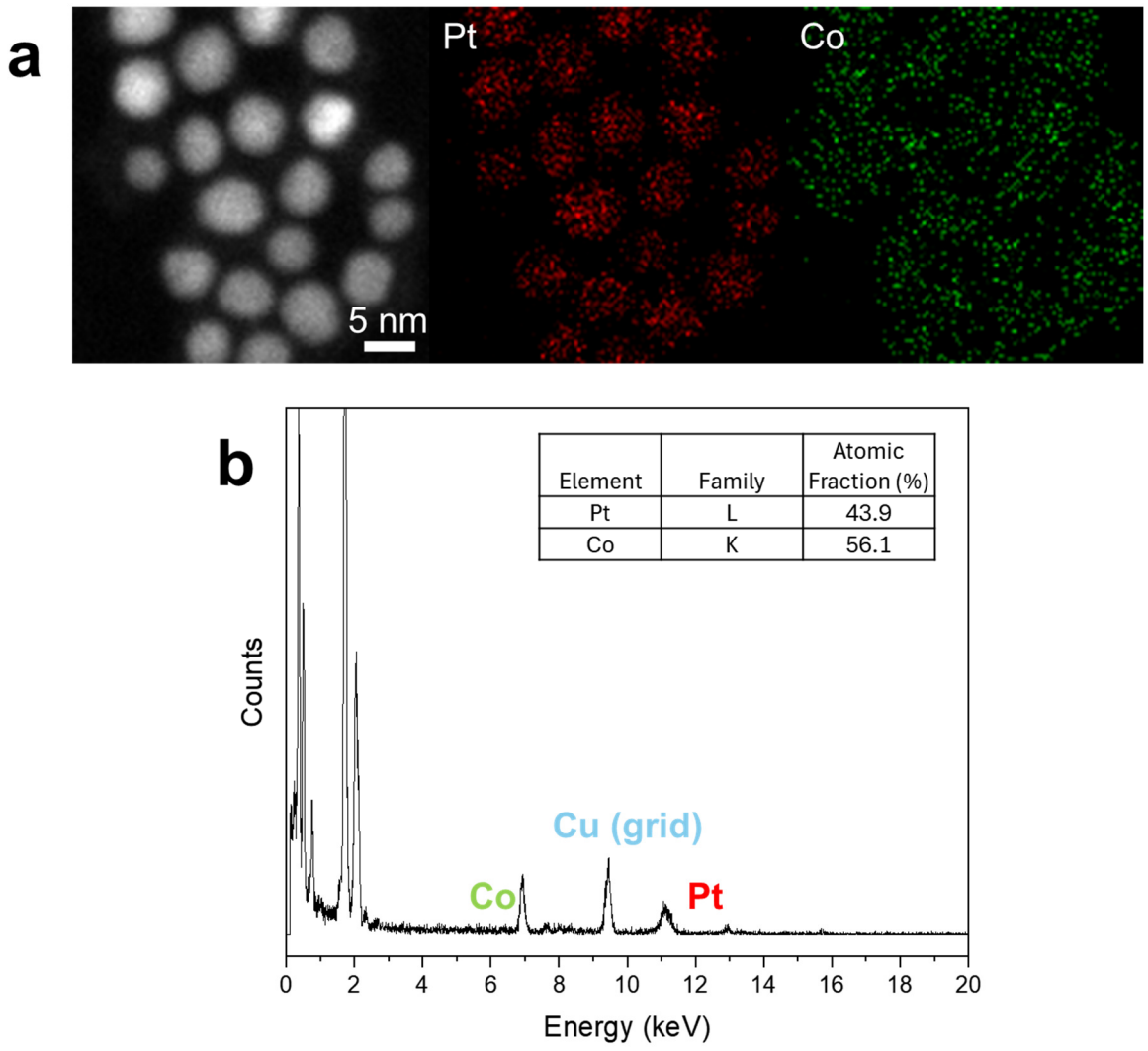

Figure S23. (a) HAADF-STEM image and corresponding EDS maps of PtCo nanocrystals. (b) Corresponding EDS spectrum with calculated atomic fraction.

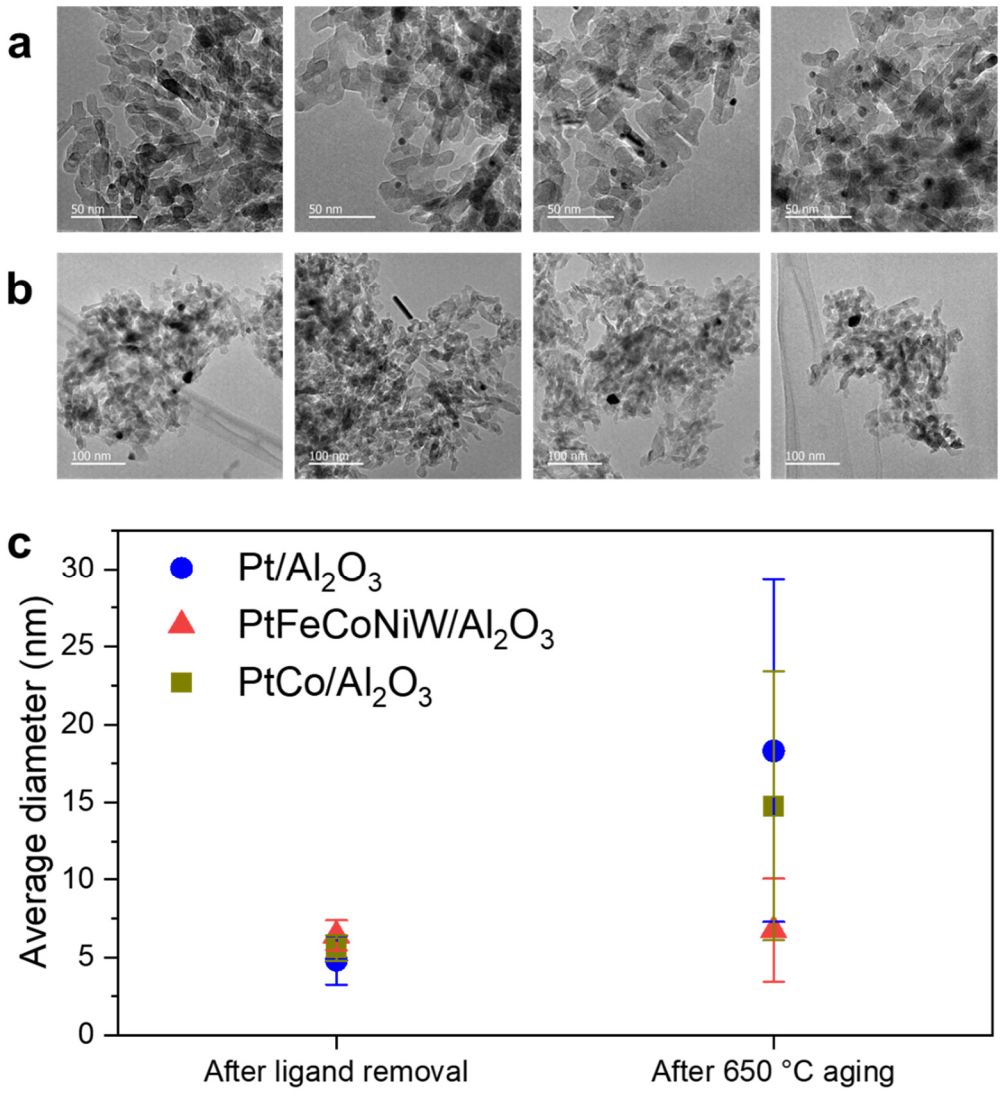

Figure S24. BF-TEM images of $PtCo/Al_2O_3$ after thermal treatment for ligand removal (a) and after hydrothermal aging at 650 °C for 6 hours (b). (c) Average nanoparticle sizes of catalysts before and after 650 °C 6 hours of hydrothermal aging.

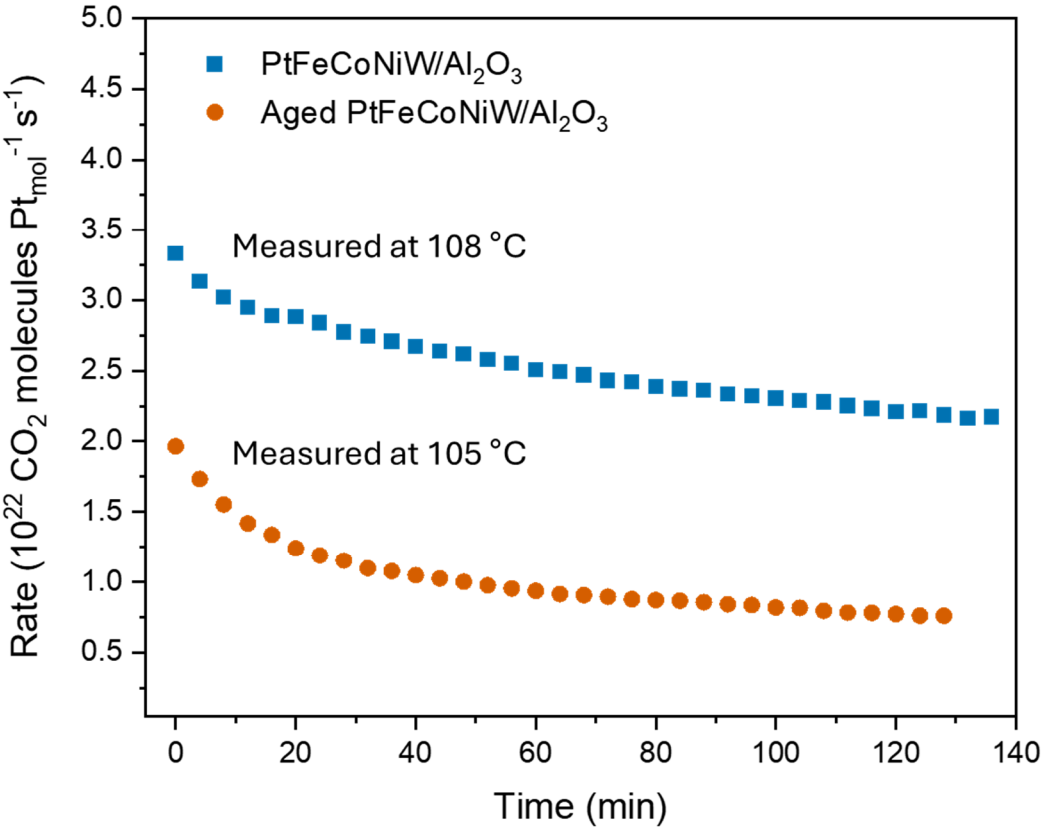

Figure S25. Initial deactivation of PtFeCoNiW/Al_2O_3 catalysts upon exposure to the reaction mixture.

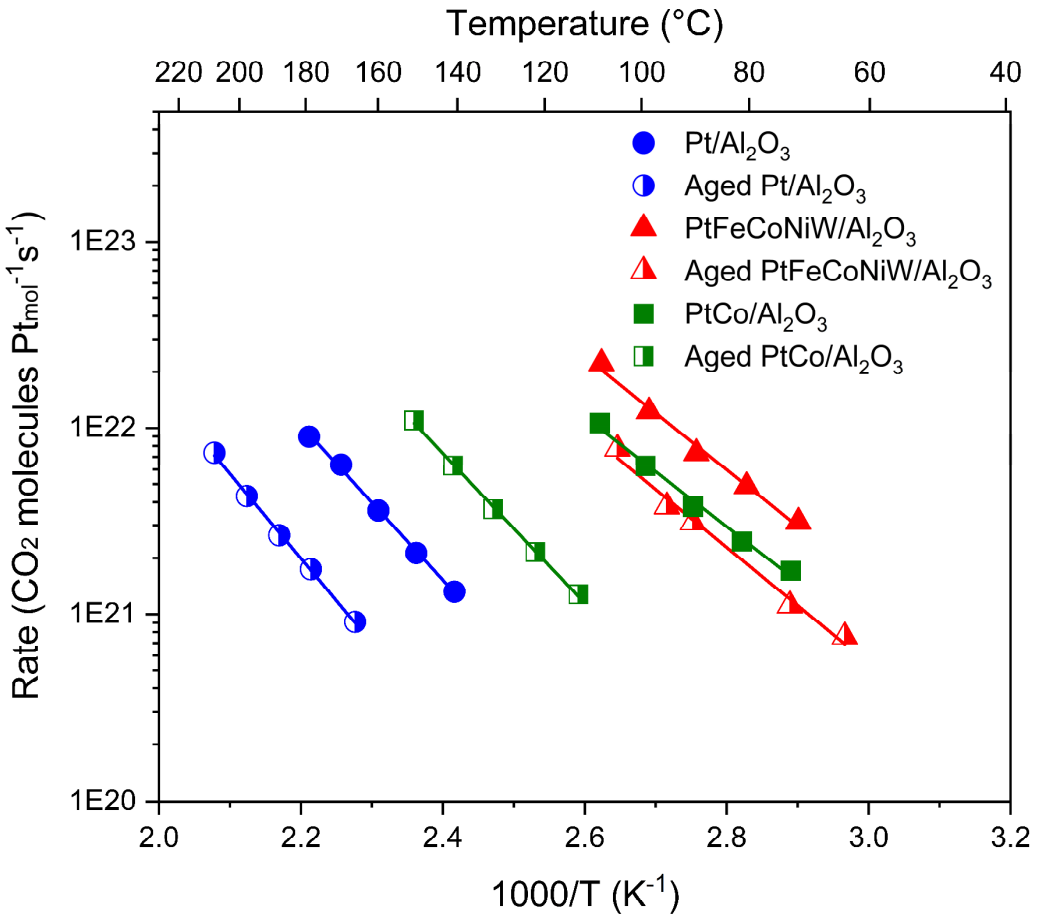

Figure S26. CO oxidation steady-state rate of Pt/Al_2O_3, $PtCo/Al_2O_3$, and $PtFeCoNiW/Al_2O_3$ before and after 650 °C 6 hours hydrothermal aging.

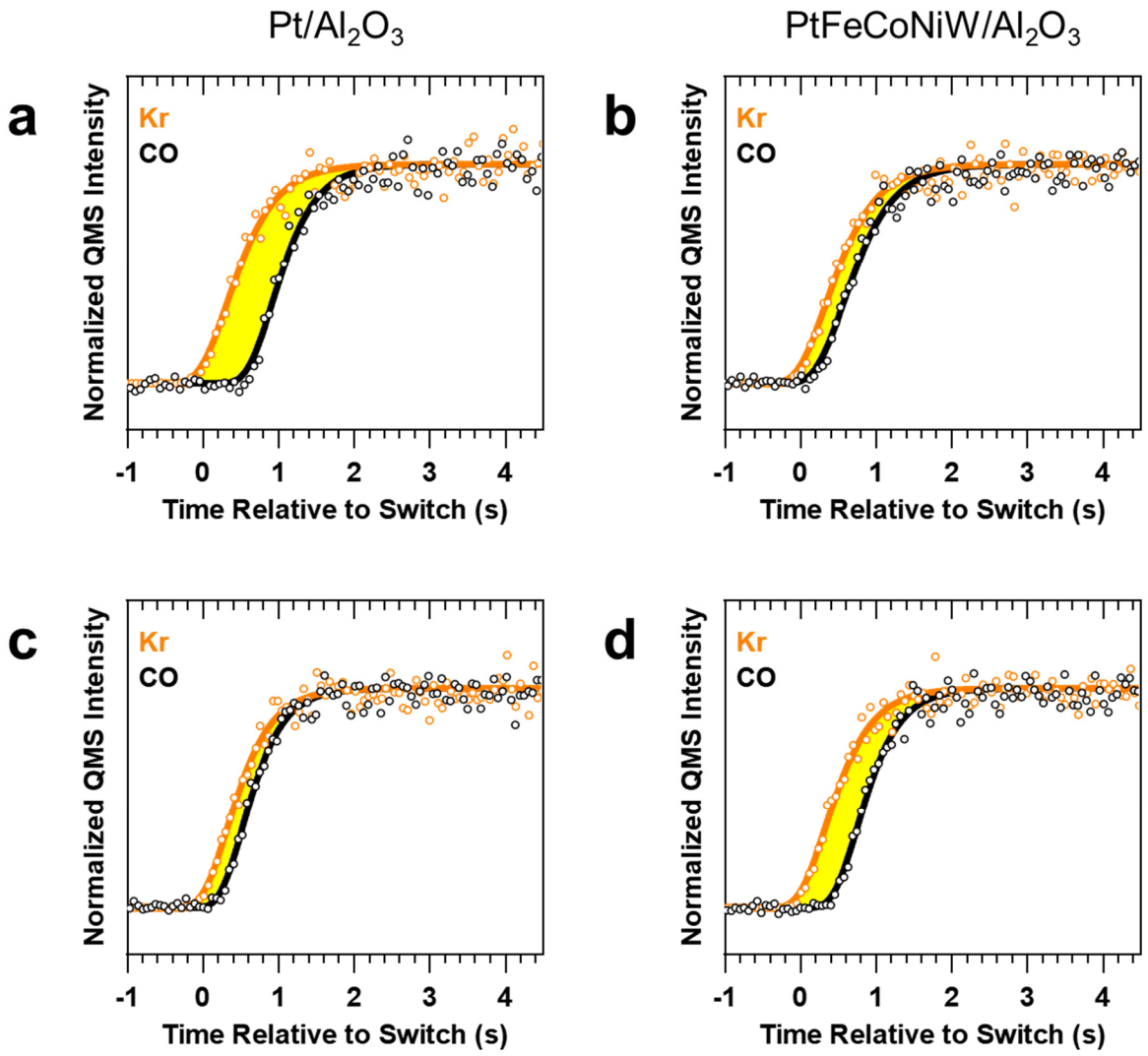

Figure S27. CO chemisorption of Pt/Al_2O_3 and $PtFeCoNiW/Al_2O_3$. CO chemisorption of after ligand removal (a) Pt/Al_2O_3 and (b) $PtFeCoNiW/Al_2O_3$. CO chemisorption of after hydrothermal aging at 650 °C for 6 h (c) Pt/Al_2O_3 and (d) $PtFeCoNiW/Al_2O_3$.

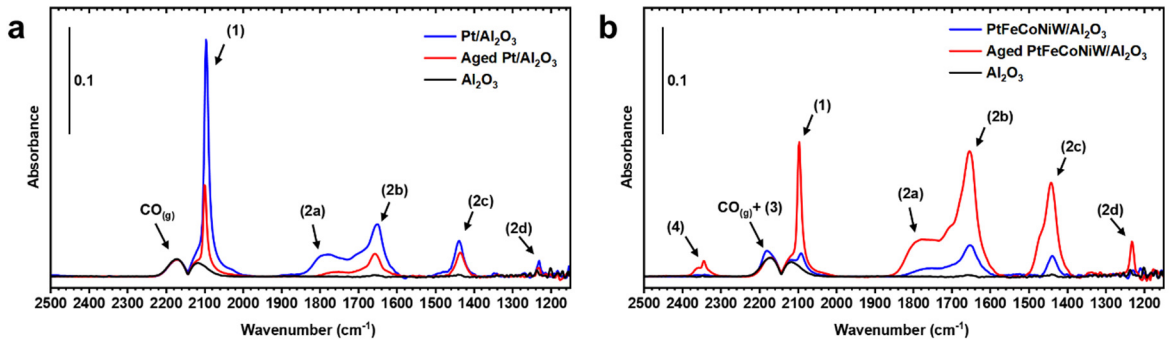

Figure S28. (a) baseline-corrected CO-DRIFTS spectra of Pt/Al_2O_3 before and after 650 °C 6 hours hydrothermal aging. (b) baseline-corrected CO-DRIFTS spectra of $PtFeCoNiW/Al_2O_3$ before and after 650 °C 6 hours hydrothermal aging.

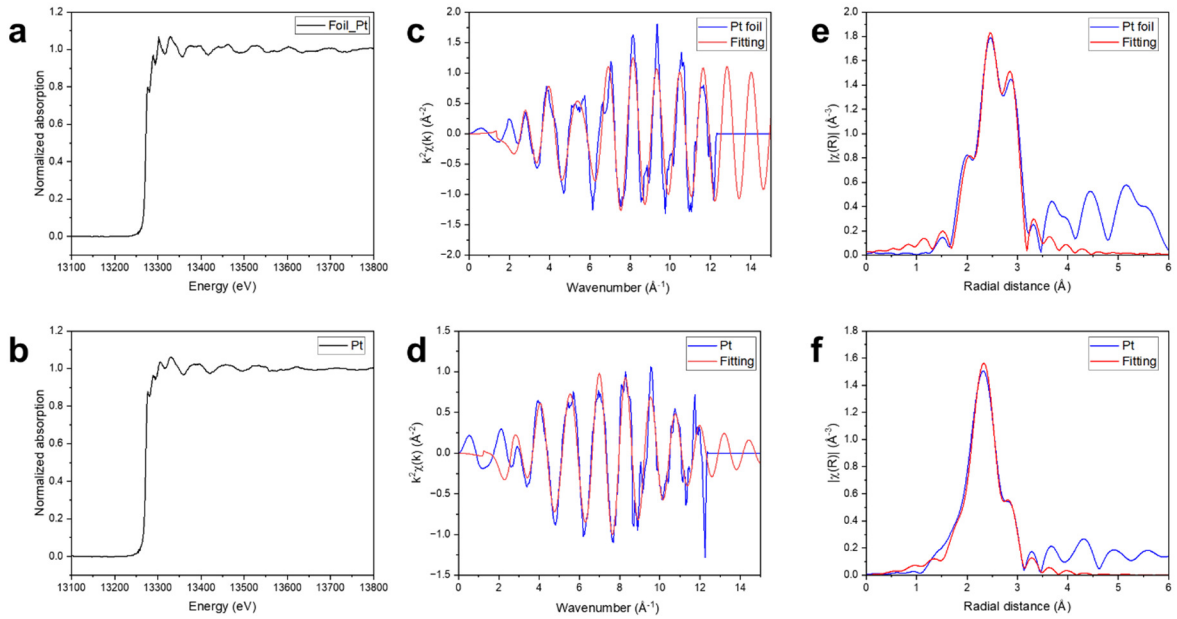

Figure S29. (a-b) XAS spectra of Pt L_2-edge of Pt foil reference (a) and PtFeCoNiW catalyst (b). (c-d) *k*-space spectra of Pt foil reference (c) and PtFeCoNiW catalyst (d) with fitting results. (e-f) R-space spectra of Pt foil reference (e) and PtFeCoNiW catalyst (f) with fitting results.

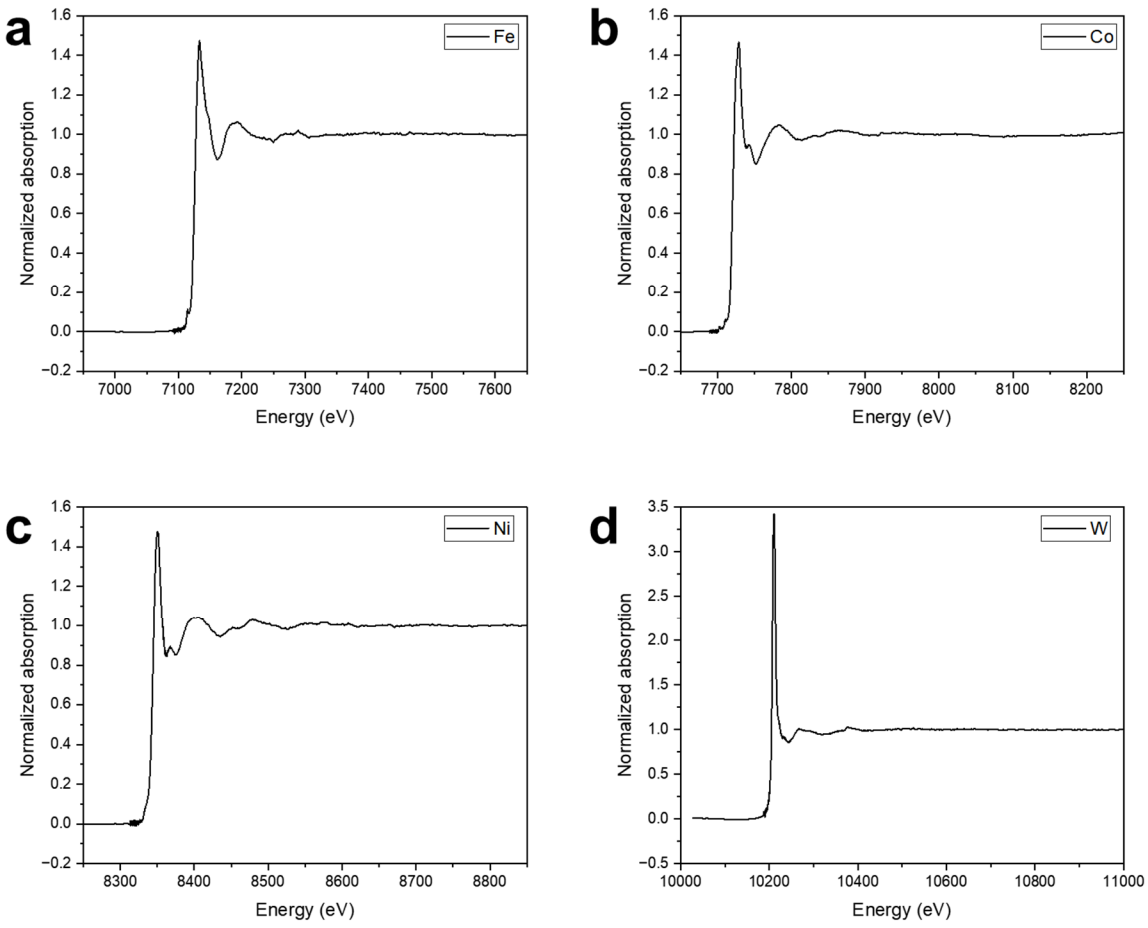

Figure S30. XAS spectra of PtFeCoNiW catalyst. (a) Fe K-edge, (b) Co K-edge, (c) Ni K-edge, and (d) W L_3-edge.

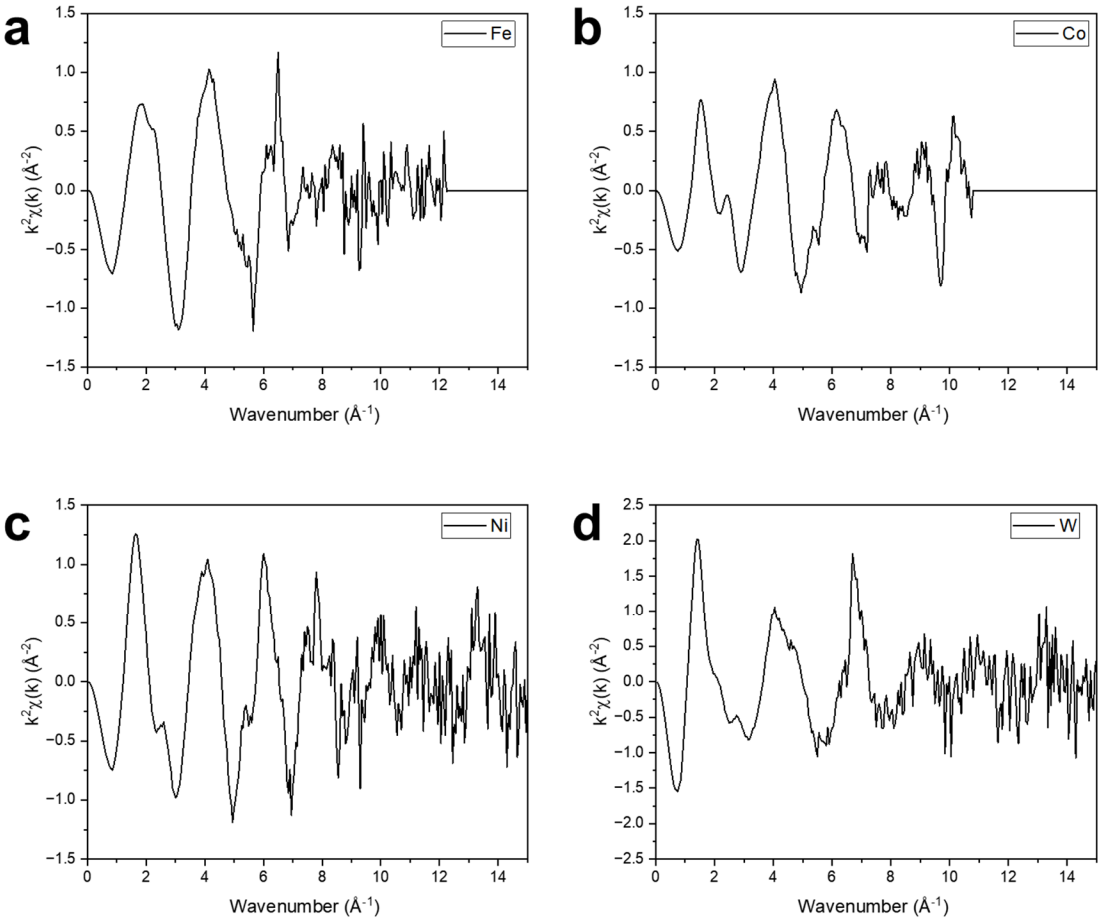

Figure S31. *k*-space spectra of PtFeCoNiW catalyst. (a) Fe K-edge, (b) Co K-edge, (c) Ni K-edge, and (d) W L_3-edge.

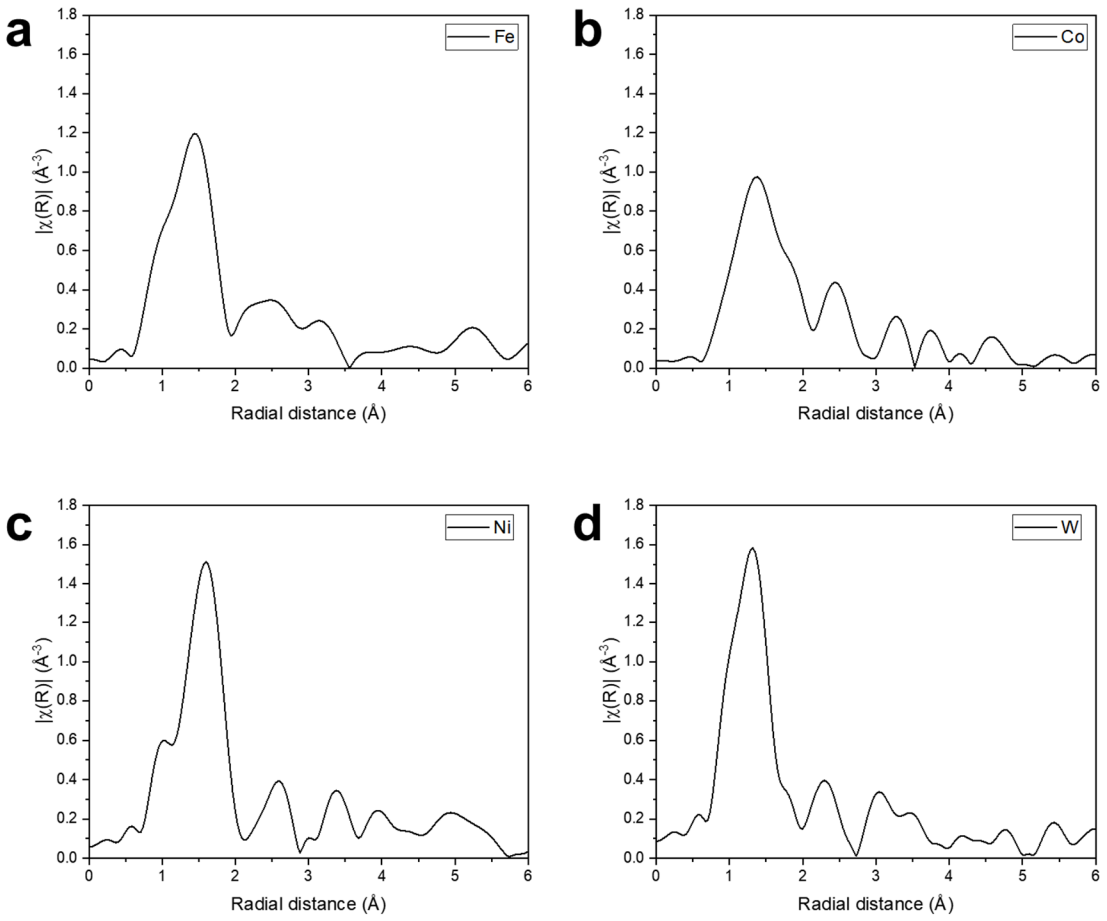

Figure S32. R-space spectra of PtFeCoNiW catalyst. (a) Fe K-edge, (b) Co K-edge, (c) Ni K-edge, and (d) W L_3-edge.

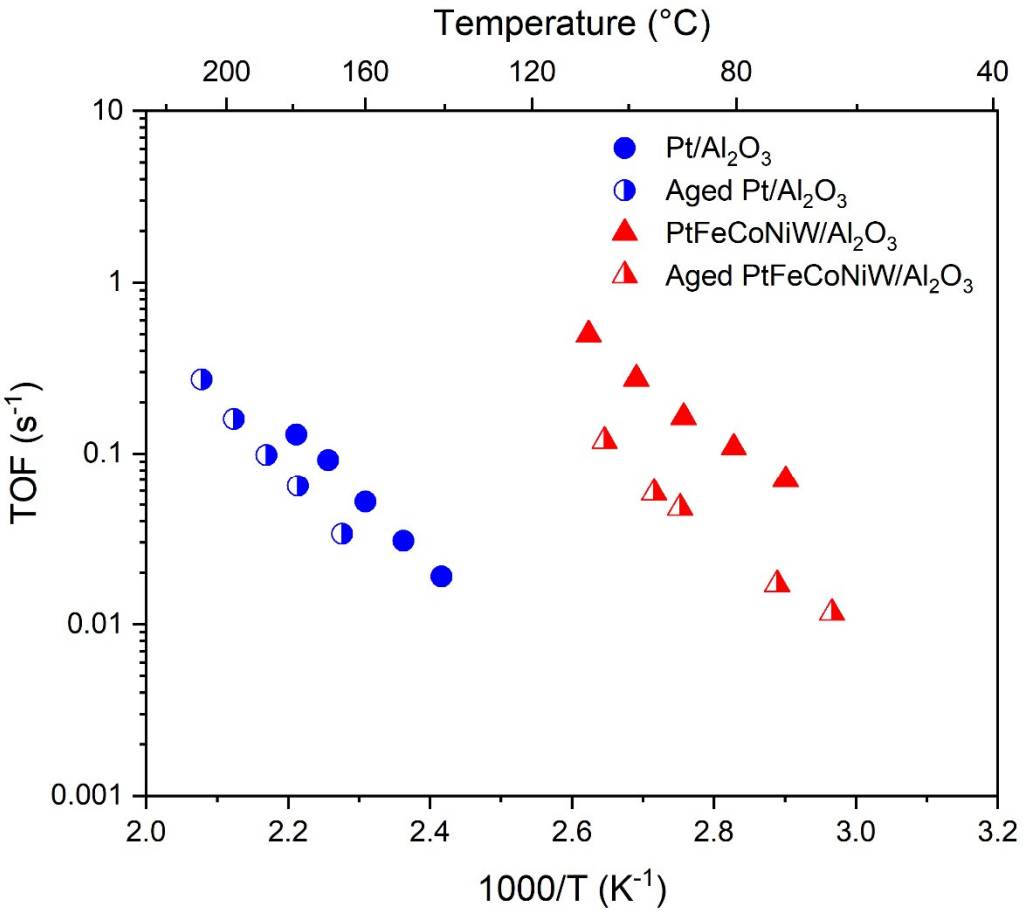

Figure S33. Turnover frequency of Pt/Al_2O_3 and $PtFeCoNiW/Al_2O_3$ before and after 650 °C, 6 6 hours of hydrothermal aging.

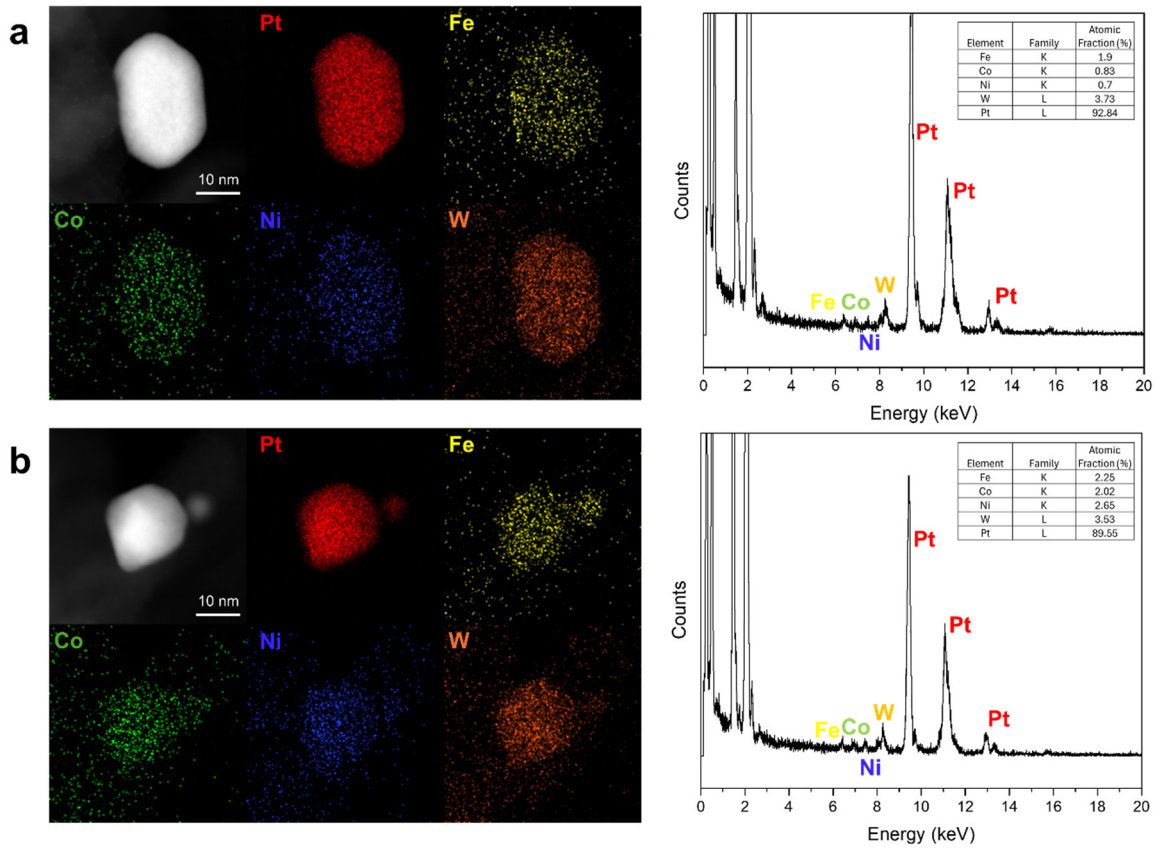

Figure S34. HAADF-STEM images and corresponding EDS maps and spectra with atomic compositions.

Composition	Mixing enthalpy (kJ mol^{-1})	Minimum average SRO	Maximum average SRO	Mean average SRO	Average SRO standard deviation	Bulk segregating atom (pair)
CoCrNiPtW	-11.2	-0.397	0.884	0.038	0.422	Co-W
CoCrFePtW	-11.2	-0.402	0.797	0.002	0.388	Co-W
CoCrMoNiPt	-13.92	-0.429	0.61	0.033	0.395	Ni-Pt
CoMoNiPtW	-12.16	-0.437	0.719	0.024	0.395	Co-Mo
CoCrFeMnPt	-12.96	-0.44	0.969	0.03	0.381	Cr-Pt
CrFeMoNiPt	-14.24	-0.453	0.735	0.022	0.392	Fe
CoFeMoPtW	-12.32	-0.46	0.692	-0.004	0.377	Fe
CrFeNiPtW	-11.84	-0.509	0.824	0.022	0.449	Fe
CoCrFeMoPt	-13.6	-0.525	0.677	-0.014	0.385	Mo-Pt
FeMnNiPtW	-11.68	-0.538	0.963	0.022	0.455	Ni-Pt
FeMoNiPtW	-12.8	-0.55	0.843	0.003	0.401	Fe
MoNiPtVW	-20.32	-0.584	0.865	0.045	0.375	Pt-V
CoCrMoPtW	-14.08	-0.607	0.914	-0.021	0.407	Cr
FeMoNiPtV	-20.32	-0.611	0.569	0.015	0.418	Pt-V
CoMoPtVW	-19.36	-0.618	0.59	0.013	0.347	Pt-V
CrMnNiPtW	-13.76	-0.619	0.541	0.032	0.396	Mn
CrFeNiPtV	-19.84	-0.62	0.634	0.02	0.481	Cr-Fe
CrFeMoPtW	-13.92	-0.624	0.896	-0.02	0.411	Mo-Pt
FeMnMoNiPt	-14.08	-0.631	0.802	0.015	0.466	Fe-Mn
CoNiPtVW	-18.24	-0.649	0.589	0.034	0.417	Co-W
FeMoPtVW	-18.56	-0.651	0.596	0.001	0.404	Pt-V
CrFeMnPtW	-12.32	-0.662	0.825	-0.024	0.428	Mn

CoMoNiPtV	-20.64	-0.668	0.542	0.027	0.391	Pt-V
MnNiPtVW	-19.68	-0.669	0.598	0.038	0.396	Pt-V
CoFeNiPtW	-8.32	-0.671	0.996	0.014	0.44	Fe
MnMoNiPtW	-14.08	-0.678	0.617	0.024	0.375	Mn
CoFeMoNiPt	-11.2	-0.695	0.996	0.016	0.45	Fe
MoPtVWZn	-15.68	-0.708	1.0	0.007	0.417	Zn
CrFeMnNiPt	-13.76	-0.709	0.967	0.049	0.444	Ni-Pt
CoFeMnPtW	-11.04	-0.711	0.678	-0.029	0.479	Pt-W
CrMoNiPtV	-21.76	-0.728	0.771	0.038	0.413	Pt-V
FeNiPtVW	-18.24	-0.73	0.67	0.013	0.466	Fe
CoCrMnPtW	-12.8	-0.74	0.691	-0.014	0.417	Mn
CuMoPtWZn	-3.2	-0.745	0.992	-0.026	0.592	Cu-Zn
CrFeMnMoPt	-14.24	-0.756	0.83	-0.033	0.463	Mn
CoFeMnMoPt	-13.44	-0.799	0.651	-0.042	0.518	Mo-Pt
CoCrMnNiPt	-13.76	-0.815	0.936	0.069	0.451	Ni-Pt
CoMnPtVW	-18.56	-0.815	0.598	-0.005	0.423	Pt-V
CoCrFeNiPt	-10.24	-0.817	0.979	0.028	0.466	Ni-Pt
CoFePtVW	-17.44	-0.844	0.554	0.006	0.377	Pt-V
CrFePtVW	-17.92	-0.86	0.829	0.007	0.418	Pt-V
FeMnPtVW	-17.44	-0.862	0.724	-0.014	0.417	Pt-V
CrMoNiPtZn	-14.72	-0.864	0.935	-0.008	0.563	Zn
CrCuPtWZn	-4.64	-0.866	0.963	-0.052	0.639	Cu
MnMoPtVW	-17.92	-0.87	0.908	-0.004	0.468	Mn
CoCrNiPtV	-20.16	-0.874	0.764	0.048	0.486	Co-Cr
CrNiPtWZn	-12.16	-0.882	0.877	0.006	0.555	Zn

CoNiPtVZn	-21.44	-0.908	0.924	0.004	0.623	Co
FeMnMoPtV	-19.04	-0.928	0.623	-0.026	0.445	Pt-V
FeMnPtVZn	-20.32	-0.938	0.896	-0.025	0.611	Pt-Zn
CoFeMoPtV	-19.52	-0.95	0.548	0.006	0.374	Pt-V
CoMnMoPtV	-20.48	-0.95	0.477	-0.01	0.449	Pt-V
CrMoNiPtW	-14.88	-0.954	0.887	0.032	0.497	Cr
CrNiPtVW	-19.84	-0.955	0.764	0.04	0.437	Pt-V
CoCrPtVW	-18.72	-0.955	0.684	-0.005	0.408	Pt-V
FeMnMoPtW	-12.8	-0.959	0.862	-0.027	0.471	Mn
CoFeMnPtV	-19.36	-0.966	0.668	-0.012	0.534	Fe-Mn
CrMoPtVZn	-18.08	-0.968	1.0	-0.049	0.562	Cr
CoMoPtVZn	-19.68	-0.972	0.799	-0.02	0.55	Zn
CrCuNiPtZn	-10.24	-0.978	0.937	0.008	0.603	Cr-Ni
CoMnMoNiPt	-14.08	-0.984	0.925	0.01	0.504	Mn
CoCrMoPtV	-20.64	-0.986	0.572	-0.006	0.42	Pt-V
CoFeMnNiPt	-11.04	-0.992	0.376	0.01	0.401	Ni-Pt
CuFeMoPtZn	-5.6	-0.993	0.795	-0.019	0.613	Fe-Mo
MnPtVWZn	-17.76	-0.998	0.917	-0.046	0.609	Zn
CoFePtVZn	-19.04	-1.009	0.889	-0.028	0.632	Pt-Zn
CrMnPtWZn	-12.48	-1.013	0.911	-0.059	0.601	Pt-Zn
CrMnPtVW	-17.92	-1.019	0.698	-0.027	0.476	Pt-V
CrFeMoPtV	-19.52	-1.022	0.853	-0.054	0.54	Pt-V
CrCuPtVZn	-14.56	-1.023	0.955	-0.036	0.682	Cr
CrNiPtVZn	-21.76	-1.024	0.962	-0.007	0.626	Cr
CrFePtWZn	-9.92	-1.026	0.875	-0.043	0.594	Zn

CrCuMoPtZn	-7.04	-1.031	0.987	-0.06	0.636	Cr
CoMnPtVZn	-22.72	-1.032	0.942	-0.032	0.646	Mn
CoCrFePtV	-18.88	-1.043	0.548	0.004	0.458	Pt-V
CoNiPtWZn	-10.24	-1.056	0.904	-0.022	0.641	Co-W
FeNiPtWZn	-9.92	-1.057	0.932	-0.026	0.646	Fe
MoNiPtWZn	-11.84	-1.057	0.969	0.003	0.572	Zn
CoCrMoPtZn	-13.6	-1.06	0.881	-0.046	0.625	Zn
CuNiPtVZn	-17.6	-1.064	0.991	0.003	0.684	Cu
FeMoNiPtZn	-12.64	-1.07	0.911	-0.018	0.639	Fe
FeMoPtVZn	-17.6	-1.072	0.874	-0.046	0.595	Zn
CrFeMoPtZn	-12.16	-1.079	0.937	-0.052	0.608	Pt-Zn
CoCuPtVZn	-16.32	-1.095	0.898	-0.031	0.674	Co-V
CrFePtVZn	-18.24	-1.097	0.908	-0.037	0.63	Zn
FeNiPtVZn	-20.16	-1.101	0.932	-0.0	0.619	Fe
FeMnPtWZn	-11.36	-1.102	0.757	-0.053	0.626	Pt-Zn
CuFePtWZn	-3.04	-1.103	0.715	-0.028	0.618	Fe-W
CrMnMoPtW	-13.76	-1.104	0.653	-0.03	0.501	Mn
MnMoPtVZn	-19.52	-1.104	0.844	-0.06	0.633	Mn
CuMnPtWZn	-7.52	-1.105	0.821	-0.037	0.662	Mn
CrMnNiPtV	-21.76	-1.105	0.657	-0.002	0.585	Mn
CuPtVWZn	-10.56	-1.106	0.982	-0.025	0.719	Cu
FeMnNiPtV	-20.32	-1.108	0.859	0.014	0.621	Fe-Mn
CoCuFeMnPt	-6.88	-1.118	0.938	-0.074	0.703	Cu-Pt
FeMnMoPtZn	-13.6	-1.12	0.725	-0.057	0.599	Pt-Zn
MnMoNiPtV	-21.6	-1.122	0.586	0.008	0.488	Mn

CoCrMnMoPt	-15.04	-1.132	0.648	-0.034	0.51	Mn
CuMoPtVZn	-12.64	-1.137	0.967	-0.038	0.71	Cu
CrMnPtVZn	-20.8	-1.14	0.953	-0.051	0.656	Zn
CoCrPtWZn	-11.04	-1.144	0.845	-0.044	0.626	Zn
FeMoPtWZn	-9.76	-1.145	0.739	-0.036	0.569	Zn
CuFePtVZn	-13.6	-1.15	0.882	-0.04	0.657	Fe
CoPtVWZn	-17.44	-1.17	0.894	-0.024	0.624	Zn
CrFeNiPtZn	-12.96	-1.173	0.954	-0.017	0.694	Fe
CrCuFePtZn	-7.04	-1.173	0.818	-0.022	0.651	Cr-Fe
FePtVWZn	-15.68	-1.175	0.855	-0.042	0.62	Zn
CoCrMnPtV	-20.48	-1.177	0.583	0.006	0.518	Pt-V
CoMnPtWZn	-12.8	-1.179	0.847	-0.046	0.643	Pt-Zn
CrMoPtWZn	-10.88	-1.18	0.999	-0.049	0.576	Zn
CoCuMoPtZn	-7.68	-1.186	0.715	-0.012	0.609	Co-Mo
CrMnMoPtZn	-14.56	-1.189	0.975	-0.085	0.69	Mn
MnNiPtWZn	-13.92	-1.194	0.901	-0.022	0.631	Mn
CoCuPtWZn	-4.8	-1.201	0.739	-0.015	0.618	Co-W
CoMoNiPtZn	-13.28	-1.204	0.86	-0.018	0.625	Pt-Zn
CrFeMnPtZn	-14.4	-1.207	0.804	-0.026	0.611	Pt-Zn
CrFeMnPtV	-19.04	-1.208	0.552	-0.003	0.485	Pt-V
CuFeMnPtZn	-10.56	-1.21	0.746	-0.024	0.63	Fe-Mn
CoMnNiPtW	-11.36	-1.21	0.913	-0.004	0.544	Mn
MnMoPtWZn	-11.68	-1.219	0.771	-0.059	0.632	Zn
CoFeMoPtZn	-11.84	-1.222	0.801	-0.028	0.594	Pt-Zn
MoNiPtVZn	-20.96	-1.224	0.968	-0.015	0.657	Zn

CrPtVWZn	-16.32	-1.229	0.995	-0.05	0.652	Zn
CoMoPtWZn	-10.88	-1.231	0.75	-0.027	0.579	Zn
CoCuFeMoPt	-4.8	-1.232	0.863	-0.051	0.642	Cu
CuFeNiPtW	-2.56	-1.233	0.907	-0.025	0.671	Cu
CoCuNiPtW	-2.56	-1.238	0.887	-0.016	0.65	Cu
CuNiPtWZn	-5.76	-1.241	0.915	0.009	0.62	Ni-W
CoCrPtVZn	-20.32	-1.255	0.914	-0.023	0.66	Zn
NiPtVWZn	-18.72	-1.255	0.965	0.004	0.616	Zn
CoCuMoNiPt	-5.6	-1.255	0.897	-0.019	0.65	Cu
CoMnNiPtV	-20.96	-1.267	0.949	0.007	0.612	Mn
CuFeMoNiPt	-5.28	-1.271	0.939	-0.032	0.678	Cu
CrMnMoNiPt	-16.0	-1.274	0.84	0.009	0.629	Mn
CoFePtWZn	-9.12	-1.283	0.868	-0.04	0.648	Pt-Zn
CuFeMnNiPt	-7.52	-1.302	0.988	-0.067	0.742	Fe-Mn
CrMnMoPtV	-19.36	-1.306	0.829	-0.061	0.666	Pt-V
CoMnMoPtW	-13.28	-1.321	0.82	-0.038	0.542	Mn
CuMoNiPtZn	-8.64	-1.328	0.861	0.008	0.635	Mo-Ni
CrCuMnPtZn	-12.0	-1.334	0.828	-0.041	0.652	Mn
CoCuMnPtZn	-12.96	-1.341	0.898	-0.045	0.709	Mn
FeMnNiPtZn	-15.36	-1.347	0.873	-0.024	0.674	Fe-Mn
CrMoPtVW	-19.04	-1.347	0.999	-0.005	0.526	Cr
CoCrCuFePt	-4.96	-1.353	0.916	-0.044	0.684	Cu
CoCrCuMnPt	-8.96	-1.361	0.902	-0.039	0.669	Cu
CoCuFePtW	-2.08	-1.367	0.882	-0.05	0.671	Cu
MnNiPtVZn	-24.16	-1.374	0.943	-0.007	0.645	Mn

CuMnPtVZn	-18.08	-1.384	0.881	-0.043	0.668	Mn
CrCuFeNiPt	-5.6	-1.387	0.987	-0.044	0.735	Cu
CoCuMnMoPt	-8.16	-1.398	0.903	-0.073	0.696	Cu
CoCrCuNiPt	-5.92	-1.419	0.926	-0.016	0.686	Cu
AgCrCuNiPt	1.76	-1.426	0.989	-0.052	0.704	Ag
CrCuMnNiPt	-9.92	-1.436	0.948	-0.036	0.701	Cu
CuMnMoPtZn	-9.92	-1.436	0.839	-0.042	0.684	Mn
CoCrCuPtZn	-9.12	-1.445	0.828	-0.011	0.667	Co-Cr
CoCrMnPtZn	-16.16	-1.446	0.892	-0.032	0.685	Pt-Zn
CrCuFeMnPt	-7.52	-1.446	0.843	-0.048	0.656	Cu
CrCuFeMoPt	-5.76	-1.447	0.871	-0.052	0.614	Cu
AgCuMoPtZn	-0.48	-1.45	0.974	-0.082	0.701	Mo
AgCuPtVZn	-10.88	-1.451	0.989	-0.059	0.704	Pt-V
CoCuMnPtW	-5.6	-1.467	0.833	-0.055	0.663	Cu
CoMnMoPtZn	-15.36	-1.481	0.908	-0.055	0.725	Mn
AgCoCuMnPt	-1.44	-1.481	0.994	-0.113	0.755	Ag
AgCoCrCuPt	2.88	-1.482	0.974	-0.071	0.737	Co-Cr
CuFeMnMoPt	-6.72	-1.488	0.851	-0.074	0.674	Cu
CoCrFePtZn	-12.0	-1.488	0.903	-0.034	0.7	Pt-Zn
CuFeMnPtW	-4.48	-1.5	0.714	-0.063	0.607	Cu
AgCrCuPtZn	-3.68	-1.502	0.936	-0.087	0.701	Cr
CuFeMnPtV	-13.44	-1.504	0.881	-0.047	0.657	Cu
CoFeMnPtZn	-14.4	-1.506	0.891	-0.054	0.711	Pt-Zn
CuMnNiPtW	-6.4	-1.513	0.914	-0.038	0.689	Cu
AgPtVWZn	-4.32	-1.522	0.999	-0.053	0.782	Ag

AgMoPtVZn	-6.88	-1.526	0.989	-0.062	0.776	Ag
CoCuMnPtV	-15.52	-1.545	0.961	-0.055	0.711	Cu
CoCuFePtV	-12.0	-1.552	0.916	-0.043	0.699	Cu
CoCrNiPtZn	-13.6	-1.565	0.888	0.002	0.691	Co-Cr
AgCoCuPtV	-4.8	-1.572	0.971	-0.082	0.748	Ag
AgCuFeMoPt	6.88	-1.573	0.987	-0.118	0.787	Ag
CoFeNiPtZn	-10.72	-1.573	0.966	-0.068	0.751	Fe
CrCuFePtW	-3.52	-1.576	0.863	-0.058	0.628	Cu
CoCuFeNiPt	-2.72	-1.588	0.992	-0.096	0.785	Fe
CoMnNiPtZn	-16.32	-1.589	0.927	-0.015	0.718	Co-Mn
CoCuMnNiPt	-8.16	-1.589	0.991	-0.045	0.759	Co-Mn
AgCrFeMoPt	3.68	-1.593	0.998	-0.117	0.749	Ag
CoCrCuMoPt	-6.88	-1.602	0.812	-0.041	0.624	Cu
AgMnPtWZn	-1.76	-1.607	0.946	-0.092	0.757	Ag
AgCoPtVZn	-11.36	-1.609	0.973	-0.082	0.757	Ag
AgCrPtVZn	-9.28	-1.622	0.995	-0.091	0.805	Cr
CuFeMoPtV	-11.2	-1.626	0.811	-0.069	0.63	Cu
AgCrCuFePt	4.96	-1.627	0.977	-0.11	0.778	Ag
AgCuMnPtV	-7.36	-1.628	0.981	-0.105	0.784	Ag
AgCuMoNiPt	3.84	-1.631	0.991	-0.047	0.723	Ag
CrMnNiPtZn	-17.44	-1.632	0.974	-0.03	0.71	Mn
AgNiPtWZn	0.32	-1.635	0.996	-0.039	0.721	Ag
AgCrPtWZn	2.08	-1.636	0.97	-0.08	0.731	Ag
AgNiPtVZn	-12.96	-1.638	0.984	-0.022	0.749	Ag
CrCuNiPtW	-5.12	-1.64	0.921	-0.018	0.669	Cu

AgMoPtWZn	4.0	-1.641	0.976	-0.055	0.767	Ag
CuMnMoNiPt	-8.96	-1.644	0.952	-0.057	0.74	Mn
AgMnPtVZn	-13.76	-1.648	0.975	-0.095	0.793	Ag
CrCuMnPtW	-5.92	-1.648	0.847	-0.071	0.631	Cu
AgMoNiPtZn	-3.04	-1.654	0.989	-0.039	0.723	Ag
AgCoCrPtZn	-3.68	-1.659	0.99	-0.054	0.806	Ag
AgCuNiPtV	-6.08	-1.66	0.952	-0.049	0.758	Ag
AgCuNiPtW	7.2	-1.66	0.99	-0.053	0.731	Ag
AgCuNiPtZn	-6.08	-1.672	0.814	-0.015	0.633	Ag
CoCrCuPtW	-4.32	-1.675	0.861	-0.051	0.652	Cu
CrCuFePtV	-11.84	-1.68	0.858	-0.038	0.688	Cu
AgFeMnNiPt	-0.16	-1.682	1.0	-0.11	0.773	Ag
AgCuFeMnPt	0.96	-1.685	0.955	-0.115	0.748	Ag
AgCoFePtZn	-1.44	-1.691	0.997	-0.116	0.859	Ag
AgCrFePtZn	-1.28	-1.697	0.952	-0.091	0.768	Ag
CoCuFePtZn	-6.88	-1.699	0.971	-0.066	0.801	Fe
AgCoCuMoPt	4.8	-1.703	0.985	-0.115	0.79	Ag
AgCoMnPtZn	-8.48	-1.71	0.998	-0.098	0.824	Ag
AgCuMnMoPt	1.76	-1.71	0.989	-0.131	0.819	Ag
AgCuPtVW	1.6	-1.712	0.998	-0.074	0.815	Ag
AgCuMoPtV	-0.96	-1.714	0.992	-0.086	0.808	Ag
AgCuMoPtW	9.92	-1.719	0.973	-0.073	0.779	Ag
CoCuNiPtV	-13.76	-1.721	0.936	-0.016	0.732	Cu
AgCoPtWZn	1.6	-1.722	0.988	-0.093	0.785	Ag
CoFeNiPtV	-17.92	-1.723	0.997	-0.008	0.671	Fe

AgCuFePtW	9.92	-1.724	0.974	-0.113	0.78	Ag
AgCrCuPtV	-3.36	-1.729	0.981	-0.096	0.806	Ag
AgCrMoPtZn	-0.8	-1.73	0.929	-0.093	0.746	Ag
CrCuMnMoPt	-8.0	-1.732	0.889	-0.095	0.723	Cu
CoCuMoPtV	-12.96	-1.733	0.864	-0.047	0.661	Cu
AgFePtWZn	3.68	-1.734	0.947	-0.093	0.759	Ag
MnMoNiPtZn	-16.48	-1.736	0.95	-0.045	0.7	Mn
AgFePtVZn	-8.32	-1.749	0.959	-0.086	0.755	Ag
AgCrCuMnPt	-0.8	-1.75	0.983	-0.123	0.796	Ag
AgCrMnPtZn	-7.2	-1.761	0.944	-0.105	0.779	Ag
AgCrCuMoPt	5.12	-1.762	0.943	-0.108	0.806	Ag
AgCoMoPtZn	-1.76	-1.766	0.964	-0.086	0.767	Ag
AgCrNiPtZn	-5.12	-1.767	0.989	-0.064	0.748	Ag
AgFeMnMoPt	1.76	-1.769	0.95	-0.124	0.789	Ag
AgCuFePtV	-2.08	-1.769	0.972	-0.101	0.771	Ag
AgFeMoPtZn	0.64	-1.773	0.986	-0.11	0.824	Ag
CrCuMoNiPt	-7.68	-1.795	0.974	-0.02	0.696	Cu
AgFeMnPtZn	-5.76	-1.796	0.929	-0.096	0.756	Ag
AgCuMnPtW	4.64	-1.802	0.952	-0.106	0.778	Ag
CuFeNiPtV	-12.8	-1.807	0.925	-0.033	0.759	Cu
AgCoFeNiPt	5.28	-1.81	0.999	-0.143	0.829	Ag
CuFeMoPtW	-3.36	-1.814	0.715	-0.064	0.645	Cu
CuMnMoPtW	-5.12	-1.817	0.68	-0.072	0.647	Cu
AgCuPtWZn	2.72	-1.823	0.998	-0.119	0.789	W
AgCoCuPtW	8.16	-1.83	0.944	-0.1	0.766	Ag

CrCuMnPtV	-14.24	-1.845	0.941	-0.07	0.732	Cu
AgCoMnNiPt	-1.12	-1.858	0.996	-0.097	0.751	Ag
AgMnMoPtZn	-4.64	-1.863	0.998	-0.131	0.906	Mn
CoCuMoPtW	-4.16	-1.865	0.754	-0.061	0.674	Cu
CuMoNiPtW	-4.8	-1.872	0.887	-0.011	0.685	Cu
AgCrFeNiPt	2.72	-1.889	0.997	-0.094	0.79	Ag
AgCrFePtV	-3.36	-1.895	0.976	-0.09	0.757	Ag
CuMnNiPtV	-16.64	-1.896	0.929	-0.05	0.791	Cu
CuMnMoPtV	-12.96	-1.91	0.804	-0.095	0.772	Cu
AgCoNiPtZn	-4.16	-1.916	0.994	-0.124	0.88	Co
AgFeMnPtV	-5.92	-1.922	0.969	-0.097	0.762	Ag
AgCrCuPtW	8.0	-1.928	0.971	-0.089	0.782	Ag
CuMoPtVW	-9.6	-1.942	0.996	-0.032	0.688	Cu
AgCoMnPtV	-8.32	-1.942	0.983	-0.108	0.796	Ag
CuFePtVW	-9.28	-1.953	0.859	-0.069	0.721	Cu
AgCoCrMoPt	2.24	-1.955	0.94	-0.117	0.765	Ag
AgCoNiPtV	-6.24	-1.959	0.966	-0.048	0.739	Ag
AgCoCrNiPt	2.08	-1.98	0.979	-0.078	0.768	Ag
AgCrMnPtV	-6.72	-1.994	0.995	-0.107	0.805	Ag
CuMnPtVW	-11.2	-1.997	0.883	-0.072	0.723	Cu
CrCuMoPtV	-12.0	-1.998	0.999	-0.059	0.731	Cu
AgCrFePtW	6.4	-2.007	0.966	-0.117	0.746	Ag
AgCoMnMoPt	0.0	-2.011	0.985	-0.118	0.812	Ag
CoCrCuPtV	-13.6	-2.016	0.936	-0.038	0.765	Cu
CuMoNiPtV	-13.92	-2.017	0.921	-0.023	0.755	Cu

AgCoCrPtV	-5.44	-2.018	0.946	-0.074	0.747	Ag
AgCrNiPtV	-6.88	-2.02	0.936	-0.032	0.722	Ag
AgCrMnMoPt	0.48	-2.021	0.997	-0.144	0.822	Ag
AgCoCrFePt	3.68	-2.021	0.972	-0.088	0.781	Ag
AgCoFePtV	-3.84	-2.024	0.981	-0.105	0.797	Ag
AgCrFeMnPt	0.48	-2.026	0.94	-0.105	0.755	Ag
CoCuPtVW	-10.72	-2.028	0.898	-0.047	0.754	Cu
AgCrMnPtW	3.04	-2.031	0.982	-0.123	0.762	Ag
AgMnNiPtV	-9.76	-2.032	0.988	-0.09	0.851	Ag
CrCuNiPtV	-14.72	-2.037	0.942	-0.02	0.757	Cu
AgCoMoPtV	-4.32	-2.048	0.893	-0.08	0.725	Ag
AgCuMnPtZn	-9.6	-2.053	0.946	-0.11	0.811	Mn
AgCoCrMnPt	-1.28	-2.061	0.981	-0.096	0.77	Ag
AgCoFeMnPt	0.8	-2.071	0.967	-0.121	0.775	Ag
AgMnPtVW	-2.72	-2.073	0.962	-0.093	0.759	Ag
AgFeMoPtV	-2.24	-2.077	0.97	-0.099	0.731	Ag
AgFeMoNiPt	3.52	-2.083	0.997	-0.091	0.811	Ag
AgCoPtVW	-1.6	-2.083	0.87	-0.065	0.734	Ag
AgCoCuFePt	5.44	-2.091	0.992	-0.161	0.906	Fe
AgFeNiPtW	6.72	-2.094	0.99	-0.084	0.787	Ag
AgCoMoPtW	5.92	-2.094	0.766	-0.075	0.712	Ag
AgFePtVW	0.16	-2.096	0.958	-0.091	0.758	Ag
AgFeMnPtW	4.48	-2.097	0.881	-0.114	0.785	Ag
AgCoCrPtW	5.28	-2.099	0.88	-0.088	0.739	Ag
AgCoMoNiPt	2.88	-2.099	0.977	-0.078	0.797	Ag

AgCoFeMoPt	4.32	-2.108	0.968	-0.111	0.809	Ag
AgFeNiPtV	-4.96	-2.11	0.996	-0.072	0.794	Ag
AgMnMoPtV	-4.96	-2.121	0.974	-0.108	0.765	Ag
AgCrMnNiPt	-2.56	-2.123	0.987	-0.085	0.782	Ag
AgFeMoPtW	7.04	-2.126	0.926	-0.1	0.752	Ag
AgCoCuNiPt	3.36	-2.143	0.989	-0.14	0.867	Co
AgMnNiPtW	1.92	-2.146	0.991	-0.09	0.813	Ag
CuNiPtVW	-11.68	-2.147	0.962	-0.028	0.805	Cu
AgMnMoNiPt	-1.12	-2.147	0.994	-0.127	0.857	Ag
AgCoFePtW	7.52	-2.148	0.971	-0.108	0.801	Ag
CuMnNiPtZn	-14.08	-2.151	0.912	-0.047	0.775	Mn
AgCoMnPtW	3.04	-2.152	0.957	-0.112	0.806	Ag
CrCuPtVW	-10.24	-2.155	0.995	-0.053	0.768	Cu
AgCoNiPtW	6.4	-2.155	0.98	-0.078	0.8	Ag
CoCuNiPtZn	-8.96	-2.159	0.86	-0.036	0.761	Co
AgMnMoPtW	4.32	-2.164	0.947	-0.109	0.788	Ag
CrCuMoPtW	-4.8	-2.177	0.999	-0.065	0.754	Cu
AgNiPtVW	-2.88	-2.18	0.983	-0.04	0.785	Ag
AgCrNiPtW	4.16	-2.185	0.847	-0.052	0.766	Ag
AgCrMoNiPt	1.12	-2.199	0.885	-0.065	0.756	Ag
AgCuMnNiPt	-2.56	-2.201	0.999	-0.144	0.881	Mn
AgCrMoPtV	-3.04	-2.202	0.949	-0.093	0.81	Ag
AgCrPtVW	-0.8	-2.215	0.954	-0.056	0.773	Ag
AgMoNiPtV	-5.6	-2.22	0.914	-0.037	0.79	Ag
AgCrMoPtW	5.6	-2.22	0.952	-0.063	0.75	Ag

AgMoNiPtW	4.96	-2.238	0.881	-0.046	0.753	Ag
AgMoPtVW	0.32	-2.239	0.999	-0.041	0.78	Ag
CuFeNiPtZn	-7.68	-2.269	0.896	-0.042	0.793	Fe
AgMnNiPtZn	-9.92	-2.3	0.993	-0.134	0.922	Mn
AgCoCuPtZn	-4.8	-2.359	0.971	-0.132	0.908	Co
AgCuFeNiPt	4.64	-2.364	0.996	-0.157	0.944	Fe
AgCuFePtZn	-1.76	-2.39	0.981	-0.134	0.912	Fe
AgFeNiPtZn	-2.56	-2.422	0.997	-0.142	0.97	Fe

Table S1. High-throughput screening results with HEA compositions sorted by minimum average SRO.

Elements	Pt	Co	Ni	Cu	Zn	PtCoNiCuZn
Lattice constant (Å)	3.9231	3.5447	3.5238	3.615	3.85	3.69
Reference	icdd 00-004-0802	icdd 00-015-0806	icdd 00-004-0850	icdd 00-004-0836	Ref. [1]	Vegard's law

Table S2. Lattice constants of PtCoNiCuZn and each element. Vegard's law was used to calculate lattice constant of PtCoNiCuZn. In calculation, lattice constant of FCC structure of elements were used. The lattice constant of FCC Zn was adopted from the previous study[1].

			CO Uptake (μmol $g_{catalyst}^{-1}$)							CO Uptake (μmol g_{Pt}^{-1})
Sample	Pt wt. %	Mass of catalyst (mg)	Average	STDEV	Run 1	Run 2	Run 3	Run 4	Run 5	Average
Pt/Al_2O_3	0.43	22.99	2.54	0.14	2.63	2.61	2.38			591
Aged Pt/Al_2O_3	0.43	21.62	0.99	0.06	1.00	1.01	1.05	0.92		230
$PtFeCoNiW/Al_2O_3$	0.37	19.64	1.41	0.23	1.30	1.16	1.69	1.49		381
Aged $PtFeCoNiW/Al_2O_3$	0.37	18.49	2.05	0.19	1.74	2.11	2.10	2.06	2.256	554

Table S3. CO chemisorption data of Pt/Al_2O_3 and $PtFeCoNiW/Al_2O_3$ after ligand removal and after hydrothermal aging at 650 °C for 6 h.

Label	Wavenumber (cm^{-1})	Assignment
1	2105	Linear CO on Pt
2	1800,1655, 1440, 1230	Bicarbonates on Al_2O_3
3	~2180	CO on MO_X
4	2350	Physisorbed linear CO_2

Table S4. Peak assignment of CO-DRIFTS experiments in Figure 5.

Parameter	Value
ΔE (eV)	7.02 ± 0.84
S_0^2	0.95
R (Å)	2.768 ± 0.005
σ^2 (Å^2)	0.0051 ± 0.0007
k-range (Å^{-1})	2.5-11.5
r-range (Å)	1.1-3.3
k-weight	2
Reduced χ^2	40.8
R-factor	0.005

Table S5. Pt L_2-edge EXAFS fitting parameters for Pt foil.

Parameter	Value
CN Pt-Pt	7.9 ± 2.1
CN Pt-M	4.2 ± 1.8
$R_{Pt\ pre}$ (Å)	2.700 ± 0.013
$R_{M\ pre}$ (Å)	2.661 ± 0.015
$\sigma^2_{Pt\ pre}$ (Å^2)	0.0083 ± 0.0024
$\sigma^2_{M\ pre}$ (Å^2)	0.0099 ± 0.0039
ΔE (eV)	5.62 ± 0.97
S_0^2	0.95
k-range (Å^{-1})	2.5-11.5
r-range (Å)	1.6-3.2
k-weight	2
Reduced χ^2	23.1
R-factor	0.01

Table S6. Pt L_2-edge EXAFS fitting parameters for PtFeCoNiW catalyst.

Reference

1. Singh, D. & Papaconstantopoulos, D. A. Equilibrium properties of zinc. *Phys. Rev. B* **42**, 8885–8889 (1990).